

DAA/LANGLEY  
IN-18  
76873-CR  
P.65

NASA Contractor Report 178287

# **Design, Development and Fabrication Of A Deployable/ Retractable Truss Beam Model For Large Space Structures Application**

**Louis R. Adams  
Astro Aerospace Corporation  
Carpinteria, California**

**Prepared for  
Langley Research Center  
under Contract NAS1-18013**

**June 1987**

(NASA-CR-178287) DESIGN, DEVELOPMENT AND  
FABRICATION OF A DEPLOYABLE/RETRACTABLE  
TRUSS BEAM MODEL FOR LARGE SPACE STRUCTURES  
APPLICATION Final Report (Astro Aerospace  
Corp.) 64 p Avail: NTIS HC A04/MF A01

N87-25349

Unclas  
G3/18 0079459



National Aeronautics and  
Space Administration

**Langley Research Center**  
Hampton, Virginia 23665-5225

NASA Contractor Report 178287

**Design, Development and  
Fabrication Of A Deployable/  
Retractable Truss Beam Model  
For Large Space Structures  
Application**

**Louis R. Adams  
Astro Aerospace Corporation  
Carpinteria, California**

**Prepared for  
Langley Research Center  
under Contract NAS1-18013**

**June 1987**



National Aeronautics and  
Space Administration

**Langley Research Center**  
Hampton, Virginia 23665-5225

## TABLE OF CONTENTS

LIST OF SYMBOLS .....	iv
SECTION 1: INTRODUCTION .....	1
SECTION 2: DESIGN REQUIREMENTS .....	4
2.1 Overall Technical Requirements .....	4
2.2 Truss Beam Model Design Requirements .....	5
2.3 Deployment/Retraction Concept .....	5
SECTION 3: BEAM DEVELOPMENT AND ANALYSIS .....	7
3.1 Beam Structure and Performance .....	7
3.1.1 Longerons Design .....	7
3.1.1.1 Stiffness .....	7
3.1.1.2 Strength .....	9
3.1.2 Diagonal Design .....	11
3.1.2.1 Stiffness .....	11
3.1.2.2 Strength .....	13
3.2 Hinge Specification .....	14
3.2.1 Hinge Positions .....	17
3.2.2 Hinge Orientations .....	19
3.2.2.1 Longerons Hinge Orientations .....	19
3.2.2.2 Diagonal Hinge Orientations .....	21
3.2.3 Point Design .....	23
3.2.3.1 Longerons Hinge .....	23
3.2.3.2 Diagonal Hinges .....	25
3.3 Deployment Analysis .....	26
3.3.1 Longerons Strain and Moment .....	26
3.3.2 Diagonal Strain and Moment .....	28
3.3.3 Deployment Forces and Energy .....	34
3.4 Hinge Design and Test Studies .....	35
3.4.1 Hinge Design .....	37
3.4.2 Test .....	37
3.4.3 Diagonal Midspan Hinges .....	40
SECTION 4: TRUSS BEAM DESIGN, FABRICATION AND ASSEMBLY .....	42
4.1 Materials .....	42
4.2 Fixtures .....	42
4.3 Bonding Procedures .....	43
4.4 Tests .....	43
4.4.1 Tube Acceptance Tests .....	43
4.4.2 Member Proof Tests .....	47
4.5 Assembly .....	48
SECTION 5: SUMMARY, CONCLUSIONS AND RECOMMENDATIONS .....	54
5.1 Summary .....	54
5.2 Conclusions .....	54
REFERENCES .....	56

## LIST OF TABLES AND FIGURES

TABLE 1:	GROUND BEAM GEOMETRY .....	24
Figure 1.	Two-bay model of a 1.4-m-diameter articulated Astromast ...	2
Figure 2.	Beam stiffness and strength .....	8
Figure 3.	Truss beam deployment .....	15
Figure 4.	Longeron packaging geometry .....	16
Figure 5.	Diagonal packaging geometry .....	18
Figure 6.	Longeron hinge specification .....	20
Figure 7.	Diagonal hinge specification .....	22
Figure 8.	Longeron twisting and bending strain .....	27
Figure 9.	Longeron bending and twisting strains and moments .....	29
Figure 10.	Diagonal strain determination .....	30
Figure 11.	Diagonal 1 bending and twisting strains and moments .....	32
Figure 12.	Diagonal 2 bending and twisting strains and moments .....	33
Figure 13.	Forces and energy .....	36
Figure 14.	Longeron compliance test .....	38
Figure 15.	Compliance test results showing necessity for close fits and low friction.....	39
Figure 16.	Diagonal hinge .....	41
Figure 17.	Batten bonding fixture .....	44
Figure 18.	Longeron bonding fixture .....	45
Figure 19.	Diagonal hinge and tube alignment .....	46
Figure 20.	Member proof tests .....	49
Figure 21.	Preamsembled beam parts .....	50
Figure 22.	Assembled beam, packaged .....	51
Figure 23.	Partial deployment of assembled beam .....	52
Figure 24.	Full deployment of assembled beam .....	53



# LIST OF SYMBOLS

<u>SYMBOL</u>	<u>DESCRIPTION</u>	<u>UNITS</u>
$A_d$	diagonal area	$m^2$
$A_\ell$	longeron area	$m^2$
$c_d$	diagonal total fitting compliance	$m/N$
$c_\ell$	longeron total fitting compliance	$m/N$
$d$	diagonal length	$m$
$d_n$	diagonal n length	$m$
$d_1$	diagonal 1 length	$m$
$d_2$	diagonal 2 length	$m$
$E$	graphite/epoxy tensile modulus	$N/m^2$
$E_{bay}$	single bay flexural energy	$J$
$EA_d$	diagonal strut stiffness	$N$
$\overline{EA}_d$	effective diagonal stiffness	$N$
$EA_\ell$	longeron strut stiffness	$N$
$\overline{EA}_\ell$	effective longeron stiffness	$N$
$EI$	beam bending stiffness	$Nm^2$
$EI_d$	diagonal bending stiffness	$Nm^2$
$EI_\ell$	longeron bending stiffness	$Nm^2$
$\hat{e}_1$	packaged centerline vector	
$\hat{e}_1'$	deployed centerline vector	
$\hat{e}_2$	packaged reference vector	
$\hat{e}_2'$	deployed reference vector	
$F_a$	axial deployment force	$N$
$F_r$	radial deployment force	$N$

# LIST OF SYMBOLS (Continued)

<u>SYMBOL</u>	<u>DESCRIPTION</u>	<u>UNITS</u>
$f$	strut frequency	Hz
$f_{\text{bend}}$	beam bending frequency	Hz
$f_{\text{tors}}$	beam torsional frequency	Hz
$G$	torsional modulus	N/m <sup>2</sup>
$GK$	beam torsional stiffness	Nm <sup>2</sup>
$GK_d$	diagonal torsional stiffness	Nm <sup>2</sup>
$GK_l$	longeron torsional stiffness	Nm <sup>2</sup>
$\vec{H}$	hinge vector	
$\vec{H}_{d1}$	diagonal 1 hinge vector	
$\vec{H}_{d2}$	diagonal 2 hinge vector	
$\vec{H}_l$	longeron hinge vector	
$I$	areal moment	m <sup>4</sup>
$ID_d$	diagonal inner diameter	m
$ID_l$	longeron inner diameter	m
$I_l$	longeron areal moment	m <sup>4</sup>
$J_a$	beam axial rotational inertia	kg m <sup>2</sup>
$J_r$	beam root rotational inertia	kg m <sup>2</sup>
$L$	beam length	m
$l$	baylength	m
$l$	strut length	m
$l_{ac}$	midhinge reference length	m
$l_{bd}$	midhinge reference length	m
$M$	bending or torsional moment	Nm
$Mar$	beam margin of strength	

# LIST OF SYMBOLS (Continued)

<u>SYMBOL</u>	<u>DESCRIPTION</u>	<u>UNITS</u>
$M_b$	beam bending strength	Nm
$M_{bd}$	diagonal bending moment	Nm
$M_{bd1}$	diagonal 1 bending moment	Nm
$M_{bd2}$	diagonal 2 bending moment	Nm
$M_{b\ell}$	longeron bending moment	Nm
$M_{br}$	required beam bending strength	Nm
$M_c$	diagonal midhinge spring moment	Nm
$M_d$	diagonal midhinge moment	Nm
$M_t$	beam torsional strength	Nm
$M_{td}$	diagonal torsional moment	Nm
$M_{td1}$	diagonal 1 torsional moment	Nm
$M_{td2}$	diagonal 2 torsional moment	Nm
$M_{t\ell}$	longeron torsional moment	Nm
$m_{tip}$	beam tip mass	kg
$m'$	beam lineal mass	kg/m
$m'$	strut lineal mass	kg/m
$OD_d$	diagonal outer diameter	m
$OD_\ell$	longeron outer diameter	m
$P$	strut load	N
$P_d$	diagonal hinge position triplet	m
$P_{Eu_d}$	diagonal Euler buckling load	N
$P_{Eu_\ell}$	longeron Euler buckling load	N
$P_\ell$	longeron hinge position triplet	m
$R$	beam circumscribed radius	m

# LIST OF SYMBOLS (Continued)

<u>SYMBOL</u>	<u>DESCRIPTION</u>	<u>UNITS</u>
$R_d$	diagonal bending radius	m
$R_g$	beam radius of gyration	m
$R_\ell$	longeron bending radius	m
$r_d$	diagonal radius	m
$r_\ell$	longeron radius	m
$s$	diagonal midhinge displacement	m
$t_d$	diagonal hinge offset	m
$t_\ell$	longeron hinge offset	m
$\begin{matrix} u \\ v \\ w \end{matrix} \}$	vector coordinate system	
$\begin{matrix} x \\ y \\ z \end{matrix} \}$	position coordinate system	m
$y$	strut deflection	m
$\alpha$	rotational acceleration	rad/sec <sup>2</sup>
$\alpha$	midhinge reference angle	degrees
$\beta$	batten-diagonal deployed angle	degrees
$\beta$	midhinge reference angle	degrees
$\Delta E$	change in flexural energy	J
$\Delta E_{\text{bay}}$	change in flexural energy of bay	J
$\Delta s$	change in diagonal displacement	m
$\Delta z$	change in bay height	m
$\Delta \phi$	change in angle	radians
$\Delta \phi_{bd1}$	change in diagonal 1 bend angle	radians

# LIST OF SYMBOLS (Concluded)

<u>SYMBOL</u>	<u>DESCRIPTION</u>	<u>UNITS</u>
$\Delta\phi_{bd2}$	change in diagonal 2 bend angle	radians
$\Delta\phi_{bl}$	change in longeron bend angle	radians
$\Delta\phi_{td1}$	change in diagonal 1 twist angle	radians
$\Delta\phi_{td2}$	change in diagonal 2 twist angle	radians
$\Delta\phi_{tl}$	change in longeron twist angle	radians
$\epsilon_{bd}$	diagonal bending strain	
$\epsilon_{bl}$	longeron bending strain	
$\epsilon_{td}$	diagonal torsional strain	
$\epsilon_{tl}$	longeron torsional strain	
$\gamma_1$	diagonal packaging angle	degrees
$\gamma_2$	diagonal packaging angle	degrees
$\gamma_3$	diagonal packaging angle	degrees
$\theta_1$	longeron angle from vertical	degrees
$\phi$	longeron packaging angle	degrees
$\phi_{bd}$	diagonal bend angle	radians
$\phi_{bl}$	longeron bend angle	radians
$\phi_{td}$	diagonal twist angle	radians
$\phi_{tl}$	longeron twist angle	radians

## SECTION 1

### INTRODUCTION

Future space missions are anticipated to require large truss platforms and beams for a number of structural applications. To control these large structures in space and understand the dynamic interaction between components, analytical models must be developed. Accurate analytical models, however, are difficult to define and are very resource intensive for the following reasons:

- The large physical size of the proposed platform and beams
- The need for detail modeling of all design features
- Variations in material properties
- Geometric variations due to manufacturing tolerances
- The large number of dynamic degrees of freedom

A program is underway within NASA named Control of Flexible Structures (COFS) to develop methods to characterize large space structures and overcome some of these difficulties. To gain some initial insight, it is desirable to perform a ground test program on a flight-quality deployable/retractable truss beam. Since the objective is to characterize a space flight beam, with response and structural performance characteristic of basic large space structures, a truss beam model was designed and fabricated to the high standards typical of flight hardware; however, formal quality assurance and accountability procedures normally used for flight hardware were not required.

The beam concept, an Articulating Astromast, shown in Figure 1, is an improvement of a structural concept that was invented 20 years ago. An engineering model of this structure, fabricated from stainless steel tubing and using wire cable diagonals and a cylindrical deployment canister, was manufactured in 1972 as part of the preliminary development of NASA's early Space Station studies. Since that time, the design has been significantly improved. Graphite/epoxy tubing now replaces both the stainless steel tubing and the wire cables of the original design. Single-degree-of-freedom hinges and a unique folding geometry have eliminated swivel joints at the end of each bay.

ORIGINAL PAGE IS  
OF POOR QUALITY

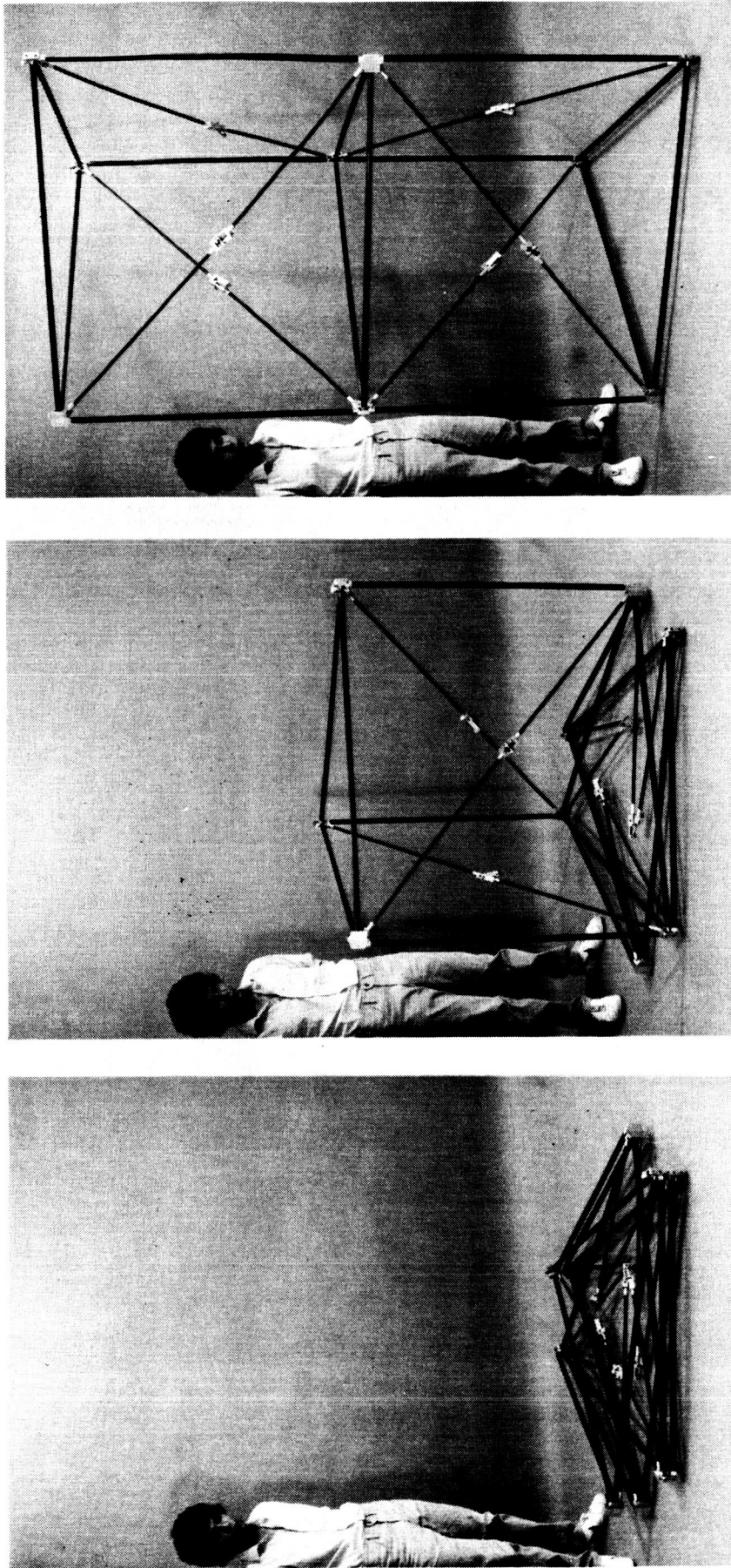


Figure 1. Two-bay model of a 1.4-m-diameter articulated Astromast.

A new hinge design which allows reliable retraction is used in the midspan of folding tubular diagonals instead of the latches originally used to tension cable diagonals. This change in diagonal design, which allows for diagonals of larger cross section, significantly increases beam torsional stiffness and strength.

This report, in various sections, reviews the design requirements for the truss beam model, describes the concept behind the beam, and includes pertinent analyses and studies concerning beam definition, deployment loading, joint compliance, etc. Design, fabrication and assembly procedures are discussed.



## SECTION 2

### DESIGN REQUIREMENTS

#### 2.1 OVERALL TECHNICAL REQUIREMENTS

The overall design requirements of the deployable/retractable truss beam model are (Reference 1):

1. High structural efficiency when evaluated on the basis of both strength and stiffness;
2. Simplicity of design and operation which shall include sequential deployment and retraction;
3. High operational reliability over many deployment/retraction cycles;
4. Design features which facilitate analytical modeling and ease of predicting structural behavior;
5. Minimum free play;
6. Design features which ensure linear response to bending, axial, and torsional loads;
7. Representative of a generic structure so that the test results will provide a basis for application to other beams of like configuration;
8. No aspects of design or fabrication which restrict its size capability;
9. No inherent or design features that would disqualify it for space applications; and
10. Easily repairable, with a high commonality of parts throughout.

The beam will be used as a ground test article for the development of research techniques in structural and dynamic characterization of large space structures. However, it shall exhibit the design, manufacturing tolerances and high performance standards typically found in a flight-rated structure. It shall be capable of remotely activated deployment and retraction, with an electrical harness and test components distributed along its length and a mass attached to the tip. The deployer, electrical harness, test components and

tip mass are not supplied under this contract. The beam is to be deployed and retracted manually. The salient features and operation of a potential deployer shall be defined and be compatible in every respect with the beam.

## 2.2 TRUSS BEAM MODEL DESIGN REQUIREMENTS

The beam delivered under this contract incorporates the following detailed aspects (Reference 1):

1. The load path through all joints and members in the deployed beam is statically determinate.
2. The beam has three parallel load-carrying members called longerons that are parallel to the beam central axis. The longerons form the apexes of an equilateral triangle when viewed as a cross section of the beam.
3. Joints are employed at locations as required to deploy and retract the beam. The number of joints is kept to a minimum and all those used in the deliverable beam are compatible with automatic deployment and retraction.
4. The longerons of the deployed beam have their centers on the circumference of a circle 1.4 meters in diameter.
5. The deployed beam has a length of approximately 20 meters.
6. The deployed beam has a minimum design bending stiffness ( $EI$ ) of  $1.15 \times 10^7$  N-m<sup>2</sup>, based on published properties of available or near-term materials, and on data obtained from tests on sample materials. The delivered beam has a minimum bending stiffness of  $0.9 \times 10^7$  N-m<sup>2</sup> when evaluated by test of a section 14 meters or longer in length.
7. The deployed beam has a design torsional stiffness equal to or greater than that required for the first torsional vibration frequency to be greater than four times the first bending frequency, both of which based on the beam to be a cantilever.
8. The deployed beam has adequate bending strength to resist failure when a 20-meter-long section mounted as cantilever with a tip mass of 35 kilograms is subjected to a rotational acceleration of 0.15 rad/sec<sup>2</sup> about a lateral axis, at the root.

## 2.3 DEPLOYMENT/RETRACTION CONCEPT

The truss beam model stows efficiently with alternating clockwise and counter-clockwise folding of the longerons toward the packaged stack. As shown in Figure 1, the diagonals must be folded in midspan to allow packaging.

The resulting design has only 36 hinge pins for 18 bays along each 20-meter-long longeron assembly. The basic packaging of the truss beam model reduces the length to 2.75 percent of its deployed value.

The beam deploys in an equally simple manner by rotating the longerons approximately 90 degrees to their upright position. As this is done, the diagonals unfold and are rigidized by spring-loaded hinges at their midspan.

There is no net rotation during either the deployment or retraction of the beam because of the alternating direction of the diagonals. All hinges have a single degree of freedom and have been designed for low compliance and minimum reduction in beam stiffness. The single-degree-of-freedom hinge lines also provide control over the kinematics of the structure during transition between the stowed and deployed configurations.

A deployment/retraction mechanism for the beam would use three synchronized leadscrews which engage threaded open-nut fittings at the longeron cluster hinge assemblies. The deployer itself is stowed and deployed using the same leadscrew mechanism to minimize the height of the package. Bays can be deployed one at a time with the assistance of a torque motor for stack rotation or two bays at a time with no necessity for stack rotation. Deployment and retraction can be continuous.

### SECTION 3

#### BEAM DEVELOPMENT AND ANALYSIS

Truss beam design is a process which involves the interaction of many factors. Bending stiffness and strength, as well as torsional stiffness and strength, are determined by member cross sections, material moduli and joint compliance. Member diameter and hinge placement are influenced by packaging requirements. Single-degree-of-freedom hinges, in general, produce strains during deployment of multi-hinged structures, and this effect must be quantified and accounted for in terms of deployment load and member size.

#### 3.1 BEAM STRUCTURE AND PERFORMANCE

Figure 2 shows a generic representation of the truss beam. The specifics of deployment kinematics do not affect this analysis. The beam is of triangular cross-section and consists of three member types: longerons which are parallel to the beam axis and provide beam stiffness and strength in bending, battens which are perpendicular to the beam axis and provide beam stability, and diagonals which are in the beam face planes and provide beam stiffness and strength in torsion and shear.

##### 3.1.1 Longeron Design

##### 3.1.1.1 STIFFNESS

The required minimum bending stiffness is

$$EI = 1.15 \times 10^7 \text{ Nm}^2$$

and in terms of longeron stiffness  $\overline{EA}_L$  and beam radius  $R$ ,

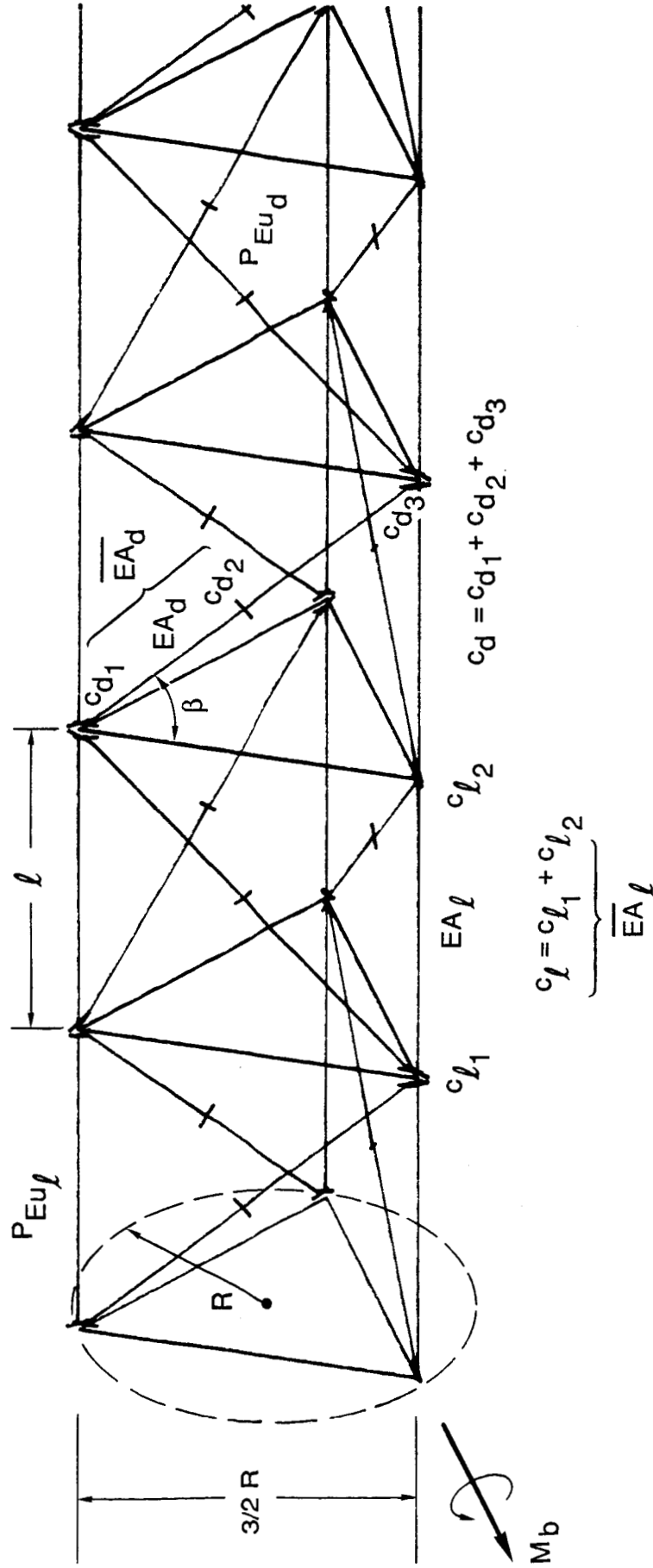
$$EI = 3/2 R^2 \overline{EA}_L$$

# BENDING

$$M_b = 3/2 R \cdot P_{Eu_l}$$

# TORSION

$$M_t = 3 \cdot R/2 \cdot P_{Eu_d} \cdot \cos \beta$$



$$EI = \frac{3}{2} R^2 \overline{EA}$$

$$GK = \frac{3}{4} R^2 \sin \beta \cos^2 \beta \overline{EA_d}$$

Figure 2. Beam stiffness and strength.

where  $\overline{EA}_\ell$  is the effective longeron stiffness including joint compliance effects:

$$\frac{1}{\overline{EA}_\ell} = \frac{1}{EA_\ell} + \frac{c_\ell}{\ell},$$

where  $EA_\ell$  is the actual longeron stiffness,  $c_\ell$  is the sum of the joint compliances on the two ends of the longeron, and  $\ell$  is the longeron length (bay length). In tests of representative joint bodies and longeron end fittings (see Section 3.4.2), a value of compliance was obtained, per hinge pin, of 0.5 microinch per pound. Then, assuming a total joint compliance of 5.7 nm/N (1.0 microinch/pound), a beam radius of  $R = 0.7$  meter, and a bay length of 1.12 meters, the effective longeron stiffness is

$$\overline{EA}_\ell = 15.6 \times 10^6 \text{ N} \quad (3.5 \times 10^6 \text{ lbf})$$

and the required longeron stiffness is

$$EA_\ell = 17.0 \times 10^6 \text{ N} \quad (3.8 \times 10^6 \text{ lbf})$$

The modulus of the selected graphite/epoxy for this application is

$$E = 1.17 \times 10^{11} \text{ N/m} \quad (17 \times 10^6 \text{ psi})$$

so that the longeron area is

$$A_\ell = 1.46 \times 10^{-4} \text{ m}^2 \quad (0.226 \text{ in}^2)$$

This is satisfied by the following cross section dimensions:

$$OD_\ell = 0.02019 \text{ m} \quad (0.795 \text{ in})$$

$$ID_\ell = 0.01491 \text{ m} \quad (0.587 \text{ in})$$

### 3.1.1.2 STRENGTH

Beam bending strength is determined by longeron Euler buckling strength. The longeron just specified has an areal moment of

$$I_{\ell} = (\pi/64) (OD_{\ell}^4 - ID_{\ell}^4) = 5.73 \times 10^{-9} \text{ m}^4$$

so that its bending stiffness is

$$EI_{\ell} = 671 \text{ Nm}^2$$

and its Euler buckling load is

$$\begin{aligned} P_{Eu_{\ell}} &= \pi^2 EI_{\ell} / \ell^2 \\ &= 5,275 \text{ N} \end{aligned} \quad (1,172 \text{ lbf})$$

This force, acting across the altitude of the triangle defining the beam cross section, determines the beam bending strength  $M_b$ :

$$\begin{aligned} M_b &= 3/2 R P_{Eu_{\ell}} \\ &= 5,540 \text{ N-m} \end{aligned}$$

The requirement that the 20-meter beam with a 35-kilogram tip mass withstand a rotational acceleration at the root of  $\alpha = 0.15 \text{ rad/sec}^2$  corresponds to a bending strength requirement of

$$M_{b_r} = J_r \alpha$$

where  $J_r$  is the beam rotational inertia about its root as follows:

$$\begin{aligned} J_r &= m_{\text{tip}} L^2 + 1/3 m' L^3 \\ &= (35 \text{ kg})(20 \text{ m})^2 + (1/3)(3.7 \text{ kg/m})(20 \text{ m})^3 \\ &= 24,000 \text{ kg m}^2 \end{aligned}$$

then the required beam bending strength is

$$M_{b_r} = 3,580 \text{ N-m}$$

Therefore a bending strength margin is expected of

$$\begin{aligned} \text{Mar} &= (M_{b_r} - M_b)/M_b \\ &= 0.55 \end{aligned}$$

### 3.1.2 Diagonal Design

#### 3.1.2.1 STIFFNESS

Diagonal stiffness is determined by the requirement that the torsional frequency be four times the bending frequency, both in cantilever. Torsional frequency is given by beam torsional stiffness GK, axial mass moment of inertia  $J_a$ , and length L:

$$f_{\text{tors}} = 0.25 \sqrt{GK/J_a L} \quad (\text{Reference 2, Table 36, case 8b})$$

Bending frequency is given by beam bending stiffness EI, lineal mass  $m'$ , and length L:

$$f_{\text{bend}} = 0.56 \sqrt{EI/m' L^3} \quad (\text{Reference 2, Table 36, case 3B})$$

Then, since  $f_{\text{tors}}/f_{\text{bend}} = 4$ ,

$$\frac{GK}{EI} = 79 \frac{J_a}{m' L^3}$$

Beam axial mass moment of inertia  $J_a$  may be obtained by assuming a mass distribution relative to the beam axis. A large share of the mass, including longeron members and corner bodies, is along the longeron line, at  $R = 0.7$  meter. Diagonals and battens are along the triangle side, between  $R = 0.35$  meter and  $R = 0.7$  meter; diagonal hinges are at  $R = 0.35$  meter. An assumed radius of gyration of  $R_g = 0.6$  meter then yields a rotational inertia of

$$\begin{aligned} J_a &= m' L R_g^2 \\ &= 0.36 m' L \end{aligned}$$



The actual value of beam lineal mass  $m'$  does not affect the solution because it cancels out of the equation. Since beam length is  $L = 20$  meters, the required ratio of torsional and bending stiffnesses is

$$\frac{GK}{EI} = 79 \left( \frac{R_g}{L} \right)^2$$

$$= 0.071$$

Both torsional and bending stiffness can be expressed in terms of diagonal and longeron stiffness, so that

$$\frac{GK}{EI} = \frac{(3/4) R^2 \sin \beta \cos^2 \beta \overline{EA}_d}{(3/2) R^2 \overline{EA}_\ell}$$

which, for  $\beta = 42.7$  degrees, is

$$\frac{GK}{EI} = 0.183 \frac{\overline{EA}_d}{\overline{EA}_\ell}$$

Therefore, the effective diagonal stiffness must be

$$\overline{EA}_d = 0.388 \overline{EA}_\ell$$

$$= 6.06 \times 10^6 \text{ N} \quad (1.35 \times 10^6 \text{ lbf})$$

$\overline{EA}_d$  is the effective diagonal stiffness including joint compliance effects:

$$\frac{1}{\overline{EA}_d} = \frac{1}{EA_d} + \frac{c_d}{d},$$

where  $EA_d$  is the actual diagonal stiffness,  $c_d$  is the sum of the joint compliances along the diagonal, and  $d$  is diagonal length. Several elements

along the diagonal contribute to its compliance: the end hinges are not normal to the centerline, so that axial strut loading produces compliance due to bending of the fitting and motion along the pin axis, in addition to pin-hole deformation; the mid-span hinge is subject to hinge opening, in addition to bending and pin-hole deformation. Total compliance is unknown, but is assumed to be less than 100 nm/N. Assuming a total joint compliance of 95 nm/N (16.6 microinch/pound) and a diagonal length of  $d = 1.58$  meter, the required diagonal stiffness is

$$EA_d = 9.6 \times 10^6 \text{ N} \quad (2.1 \times 10^6 \text{ lbf})$$

The modulus of the selected graphite/epoxy for this application is

$$E = 1.17 \times 10^{11} \text{ N/m}^2 \quad (17 \times 10^6 \text{ psi})$$

so that the diagonal area is

$$A_d = 0.82 \times 10^{-4} \text{ m}^2$$

This is satisfied by the following cross section dimensions:

$$OD_d = 0.01511 \text{ m} \quad (0.595 \text{ in})$$

$$ID_d = 0.01115 \text{ m} \quad (0.439 \text{ in})$$

### 3.1.2.2 STRENGTH

Beam torsional strength is determined by diagonal Euler buckling strength, and therefore affects diagonal sizing; however, no requirement was placed on beam torsional strength. Beam torsional strength is given by

$$M_t = 3 P_{Eu_d} \cos \beta \quad R/2$$

Diagonal Euler buckling strength is

$$\begin{aligned}
 P_{Eu_d} &= \pi^2 EI_d / d^2 \\
 &= 833 \text{ N} \qquad \qquad \qquad (185 \text{ lbf})
 \end{aligned}$$

so that beam torsional strength is, for reference,

$$M_t = 642 \text{ N-m} \qquad \qquad \qquad (5,700 \text{ in-lbf})$$

### 3.2 HINGE SPECIFICATION

The attainment of low hinge fitting compliance requires that single-degree-of-freedom hinges are used for packaging. Figure 3 shows the truss beam with two bays in a partially deployed state, and several bays completely packaged. Longerons are hinged only at their ends; diagonals are hinged at their ends and near their centers; battens are rigidly attached to nodal bodies. In establishing the hinge design, the following constraints and/or ground rules are adhered to.

1. Each bay is the mirror image of its adjacent bay, so that only one basic type of each hinge fitting need be designed.
2. The longeron hinge-centerline angle is the same on both ends.
3. The diagonal mid-span hinge, when packaged, is in the batten plane. This is an arbitrary decision, based on practical and analytical experience, made in order to minimize deployment strain and package height.
4. The diagonal mid-span hinge, when deployed, is in the face plane. This is an arbitrary decision, based on practical and analytical experience, made in order to minimize deployment strain.
5. All deployed centerlines converge at nodal points.
6. All hinges, except for the diagonal mid-span hinge, intersect and center on associated deployed centerlines.

Specification of truss beam hinges requires the definition of two geometric characteristics for each hinge: a position and an angular orientation. The position is uniquely determined by beam concept and packaging requirements; angular orientation is governed only by the requirement that members be unstrained in packaged and deployed configurations, and therefore is variable for design. In Figure 4, a bay of the truss beam is shown in

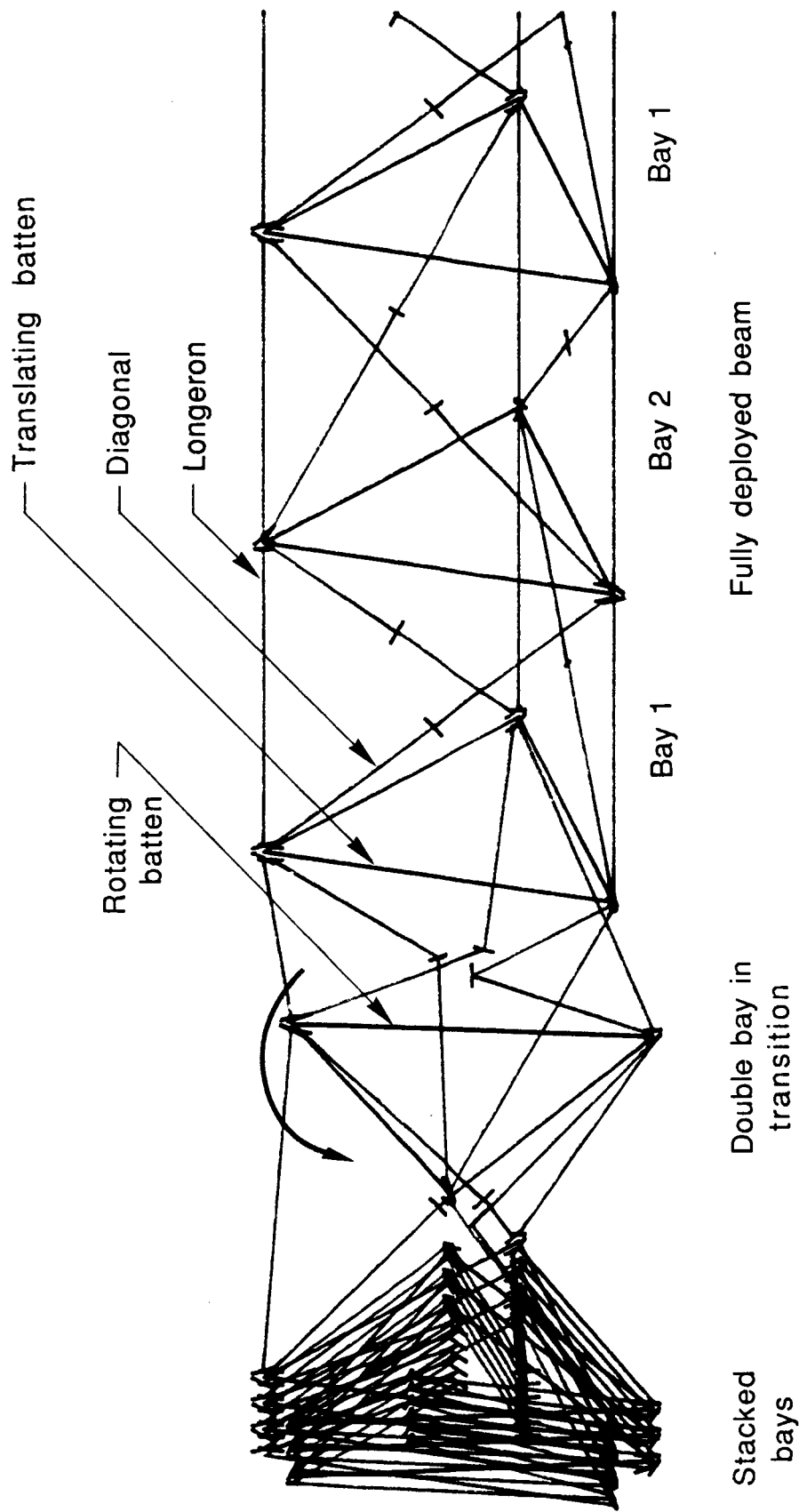


Figure 3. Truss beam deployment.

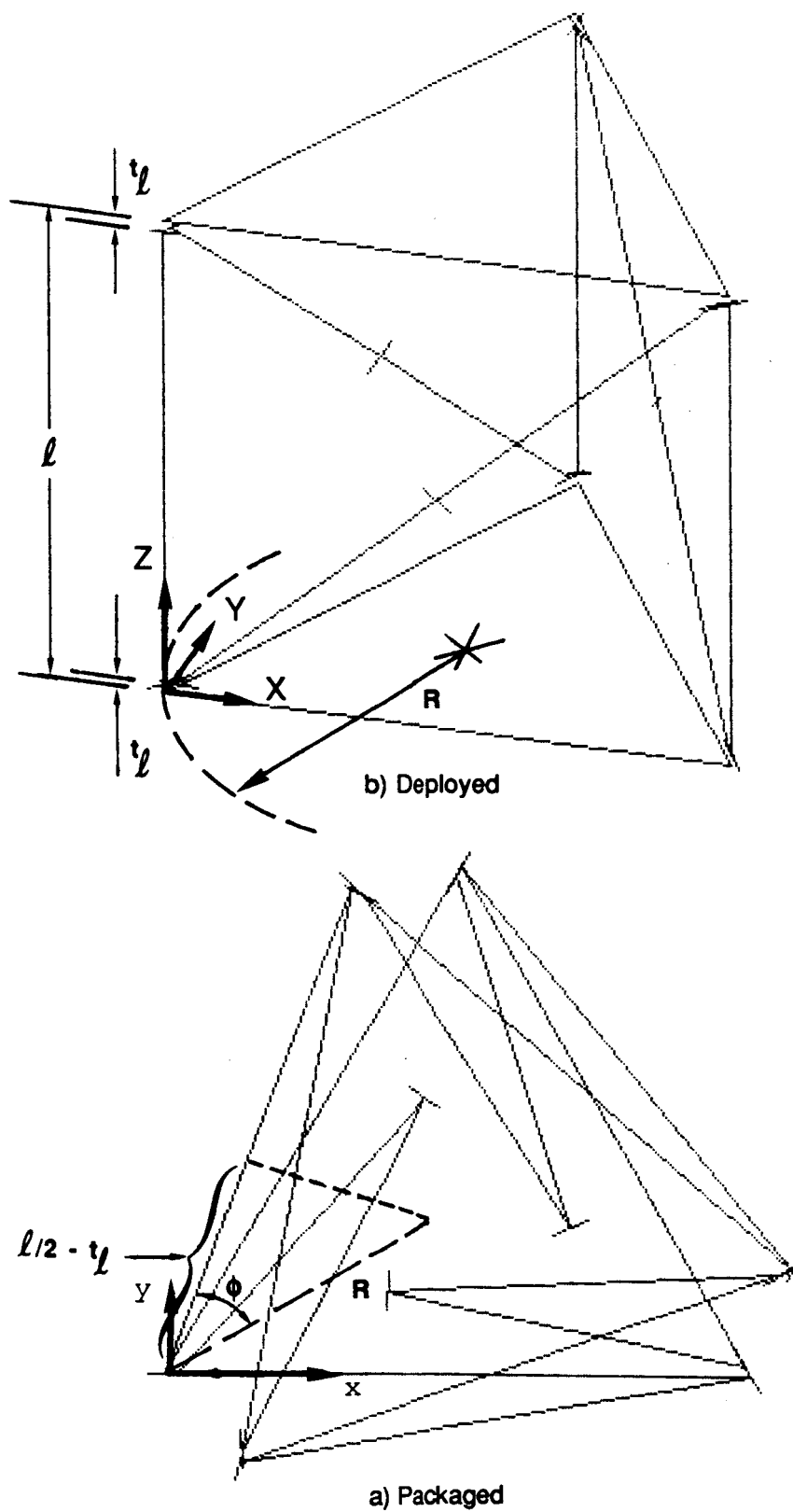


Figure 4. Longerons packaging geometry.

packaged and deployed configurations. In Figure 4(a), a Cartesian coordinate system is established, with the origin at one corner of the base batten plane, the x-axis along one batten, y in the batten plane and perpendicular to x, and z along the longeron. Point coordinates are specified by a number triplet x,y,z; hinge orientations are indicated by a triplet u,v,w, which gives the x,y,z components of a unit vector, or direction cosines.

### 3.2.1 Hinge Positions

The longeron is hinged identically at its two ends, at a vertical offset distance  $t_\ell$  above or below the adjacent batten plane. The hinge passes through and is centered on the deployed longeron centerline, so its center position is

$$x_\ell = 0$$

$$y_\ell = 0$$

$$z_\ell = t_\ell$$

or

$$P_\ell = [0, 0, t_\ell]$$

Packaged beam geometry is thus specified: the packaging angle  $\phi$  is obtained from the bay length  $\ell$ , the beam radius  $R$ , and longeron offset  $t_\ell$ , assuming the packaged longeron to be horizontal.

$$\cos \phi = \frac{\ell/2 - t_\ell}{R}$$

Diagonal end hinges pass through and are centered on the deployed diagonal centerline. The base diagonal, which when deployed lies in the x-z plane an angle  $\beta$  away from the batten direction, as shown in Figure 5, is hinged at a vertical offset distance  $t_d$  above the batten plane. Then the diagonal end hinge center position is

$$P_d = [t_d/\tan \beta, 0, t_d]$$

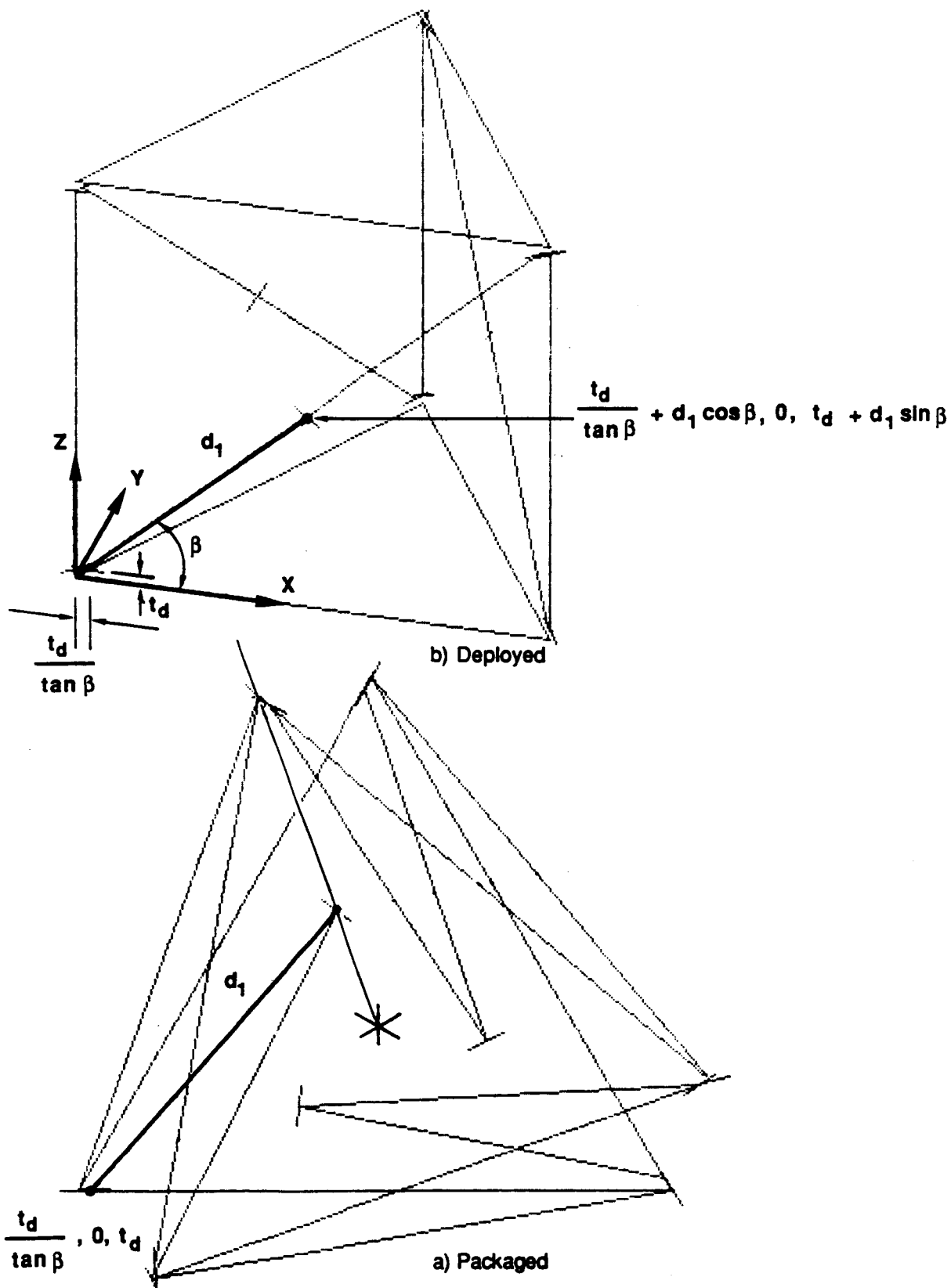


Figure 5. Diagonal packaging geometry.

The diagonal midspan hinge location is a design variable. To keep deployment strain low, the design approach adopted was to package the diagonal midspan hinge on the far side of beam center. With this position determined, beam hinge positions are specified in their entirety.

### 3.2.2 Hinge Orientations

Single-degree-of-freedom hinge axis orientations are determined by the change in orientation of two reference unit vectors associated with the rotating member. One vector,  $e_1$ , may be the centerline, and another vector,  $e_2$ , may be another hinge line, such as the diagonal mid-span hinge, or a reference direction. Then the required hinge is the cross product of the vector differences between packaged and deployed configurations.

$$\vec{H} = (\hat{e}_1' - \hat{e}_1) \times (\hat{e}_2' - \hat{e}_2)$$

The primed and unprimed vectors denote deployed and packaged orientations.

#### 3.2.2.1 LONGERON HINGE ORIENTATION

Figure 6 shows longeron vector orientations. The deployed longeron centerline is pointed upward, along the z-axis. Then

$$\hat{e}_1' = [0, 0, 1]$$

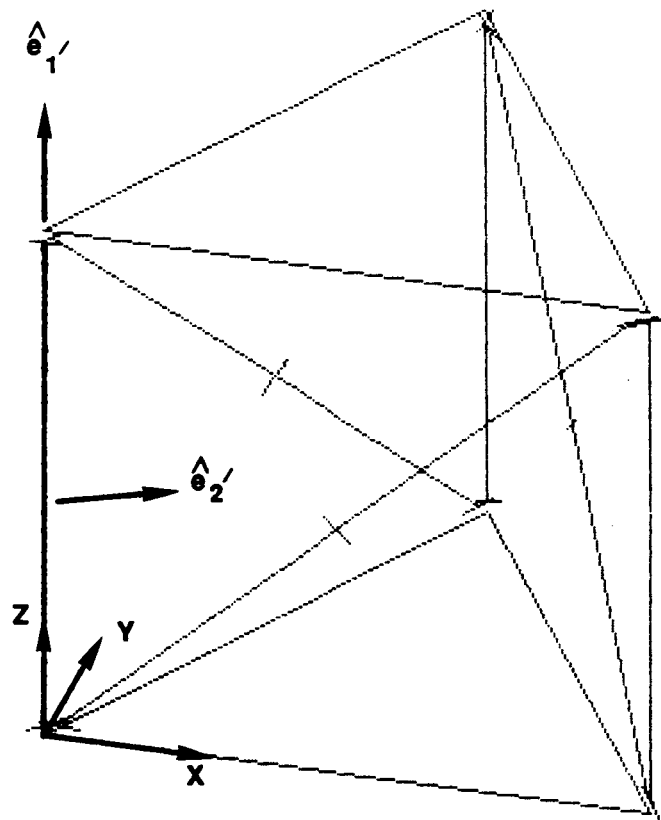
The packaged longeron centerline is in the x-y plane, at an angle of  $\phi$  plus 30 degrees with respect to the x-axis;  $\phi$  is the packaging angle defined in Section 3.2.1. Then

$$\hat{e}_1 = [\cos(\phi+30), \sin(\phi+30), 0]$$

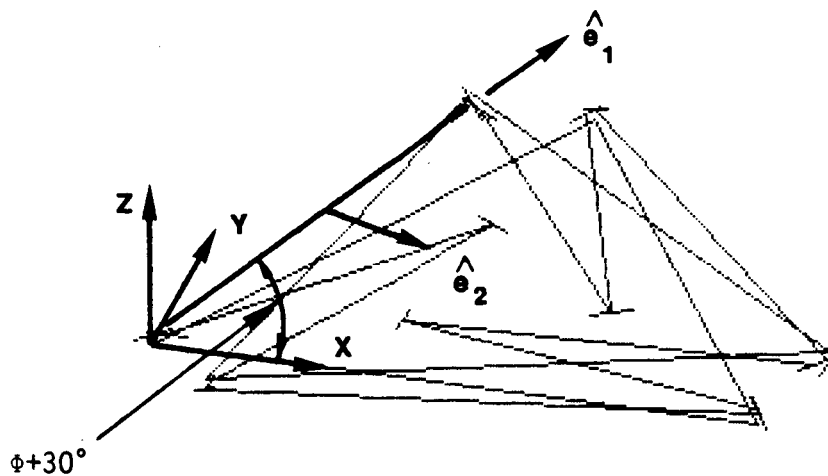
The other vector chosen for the longeron points radially inward when deployed, and packages in the x-y plane, perpendicular to the longeron line, inward. Then

$$\hat{e}_2' = [\cos(30), \sin(30), 0]$$





b) Deployed vector orientation



a) Packaged vector orientation

Figure 6. Longeron hinge specification.

and

$$\hat{e}_2 = [\sin(\phi+30), -\cos(\phi+30), 0]$$

The hinge line is

$$\vec{H}_\ell = \begin{vmatrix} \hat{i} & \hat{j} & \hat{k} \\ -\cos(\phi+30) & -\sin(\phi+30) & 1 \\ \cos(30) - \sin(\phi+30) & \sin(30) + \cos(\phi+30) & 0 \end{vmatrix}$$

which reduces to the column vector

$$\vec{H}_\ell = \begin{bmatrix} -\sin(30) - \cos(\phi+30) \\ \cos(30) - \cos(\phi+30) \\ -\cos(\phi+30) \{ \sin(30) + \cos(\phi+30) \} + \sin(\phi+30) \{ \cos(30) - \sin(\phi+30) \} \end{bmatrix}$$

### 3.2.2.2 DIAGONAL HINGE ORIENTATIONS

The diagonal does not package symmetrically; therefore, the hinge axes on the ends are not similar. Each end is considered separately. Figure 7 shows one end of the diagonal, described geometrically in Section 3.2.1. The vectors  $\hat{e}_1$  and  $\hat{e}_2$ , defining the centerline of the member and midspan hinge axes, are given, packaged and deployed, as

$$\hat{e}_1 = [\cos \gamma_1, \sin \gamma_1, 0]$$

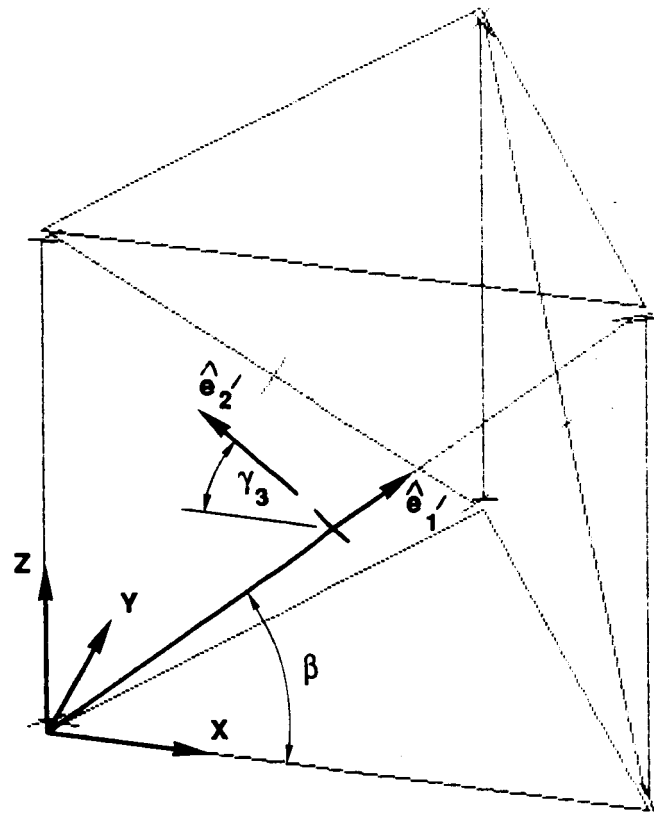
$$\hat{e}_1' = [\cos \beta, 0, \sin \beta]$$

$$\hat{e}_2 = [-\cos \gamma_2, \sin \gamma_2, 0]$$

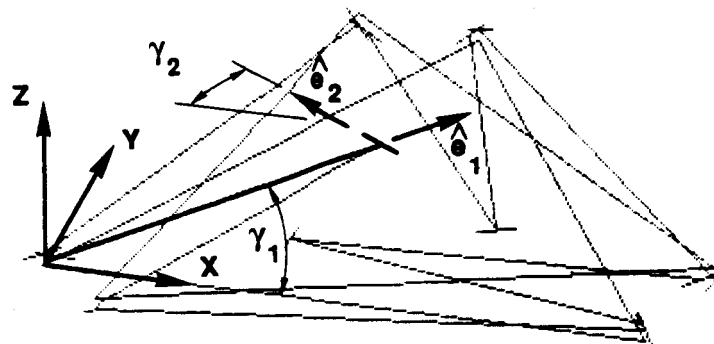
$$\hat{e}_2' = [-\cos \gamma_3, 0, \sin \gamma_3]$$

In these equations, it is implicitly assumed that

- the member centerline lies in the batten (xy) plane when packaged;
- the member centerline lies in the longeron-batten (xz) plane when deployed;



b) Deployed vector orientation



a) Packaged vector orientation

Figure 7. Diagonal hinge specification.

- the midspan hinge axis lies in the batten plane when packaged, and
- the midspan hinge axis lies in the longeron-batten plane when deployed.

Of these assumptions, only the second is required by beam geometry. The third and fourth are possible and are advantageous in terms of diagonal strain during deployment. Experience gained from prototype model evaluation and from general analyses conducted independently and during the COFS program have shown this diagonal mid-span hinge configuration to result in relatively lower diagonal strain in the truss beam. The first assumption is not strictly true and leads to a slight error in hinge orientation specification. The end hinge is

$$\vec{H}_{d1} = \begin{bmatrix} -\sin \gamma_1 \sin \gamma_3 + \sin \gamma_2 \sin \beta \\ \sin \beta (-\cos \gamma_3 + \cos \gamma_2) - \sin \gamma_3 (\cos \beta - \cos \gamma_1) \\ -\sin \gamma_2 (\cos \beta - \cos \gamma_1) + \sin \gamma_1 (-\cos \gamma_3 + \cos \gamma_2) \end{bmatrix}$$

The hinge on the other end of the diagonal,  $\vec{H}_{d2}$ , is determined by inversion of the single bay, followed by analysis similar to that above. The angles  $\gamma$ ,  $\gamma_2$ , and  $\gamma_3$  are different from, but consistent with, those for  $\vec{H}_{d1}$ .

### 3.2.3 Point Design

#### 3.2.3.1 LONGERON HINGE

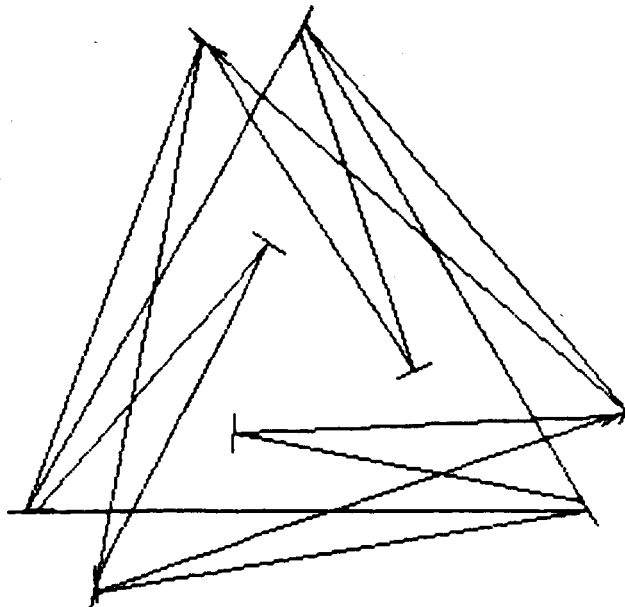
The longeron hinge axis intersects and centers on the deployed longeron centerline. It is located on the z-axis, 0.01905 meter (0.75 inch) above the batten plane. Since the bay length is  $\ell = 1.12$  meters, the packaging angle is, from Section 3.2.1,

$$\phi = \cos^{-1} \left( \frac{1.12/2 - 0.01905}{0.7} \right) = 39.395 \text{ deg}$$

Table 1 shows the longeron orientation, as determined using the equation Section 3.2.2.1.

TABLE 1: GROUND BEAM GEOMETRY

DIMENSIONS (mm):	RADIUS 700	BAYLENGTH 1120.000	PACKAGED BAY 38.100			
ANGLES (Deg):	DIAG CL - BATTEN PKG DPL 48.58729 42.73053		DIAG HINGE PKG DPL 90 0			
OFFSETS (mm):	LONG 19.050	DIAG 19.050	DIAG MID 8.467			
PROPERTIES:	E(N/m^2)		G(N/m^2)			
LONGERON	1.17E+11		4.E+9			
DIAGONAL	1.17E+11		4.E+9			
POSITION (mm)	VECTOR	ID (mm) OD (mm) AREA (mm^2)	EA (10^6 N)	EI (Nm^2)	GJ (Nm^2)	LENGTH (mm)
LONGERON:						
0.00000	.91645	14.91000				
0.00000	.07531	20.19000	17.03008	670.50015	45.84616	1081.90000
19.05000	.39301	145.55627				
DIAGONAL 1:						
20.62223	.99739	11.15000				
0.00000	.05102	15.11000	9.55577	210.60593	14.40041	768.82977
19.05000	-.05102	81.67324				
DIAGONAL 2:						
20.62223	.94867	11.15000				
0.00000	-.22364	15.11000	9.55577	210.60593	14.40041	825.68687
19.05000	.22364	81.67324				



### 3.2.3.2 DIAGONAL HINGES

The diagonal end hinge axes intersect and center on the deployed diagonal centerline, at a distance of  $t_d = 0.01905$  meter (0.75 inch) above the batten plane. The deployed centerline is directed by the vector  $(\cos \beta, 0, \sin \beta)$ , where

$$\beta = \tan^{-1} \left( \frac{l}{\sqrt{3} R} \right) = 42.7305 \text{ deg}$$

End hinge axis orientations are determined by the various angles in Section 3.2.2.2.

#### 3.2.3.2.1 Diagonal 1

Referring to Figure 7, the angles for the point design are, for diagonal 1,

$$\gamma_1 = 48.58692 \text{ degrees}$$

$$\gamma_2 = 34.41193 \text{ degrees}$$

$$\gamma_3 = 40.26832 \text{ degrees}$$

The orientation for diagonal 1, given in Table 1, is the solution of the equations of Section 3.2.2.2, using the above angles.

#### 3.2.3.2.2 Diagonal 2

The angles for the point design are, for diagonal 2,

$$\gamma_1 = 16.20152 \text{ degrees}$$

$$\gamma_2 = 66.79732 \text{ degrees}$$

$$\gamma_3 = 40.26832 \text{ degrees}$$

The orientation for diagonal 2, given in Table 1, is the solution of the equations of Section 3.2.2.2, using the above angles.

### 3.3 DEPLOYMENT ANALYSIS

Straining occurs in general during deployment of a multi-hinged structure which is unstrained at the extremes of full deployment and full packaging. The straining is the result of the inability of a set of rigid body rotations of component struts to simultaneously satisfy the angular requirements of all hinges. In effect, a hinge orientation may be different as defined by a strut end and by the feature to which the strut is attached. Therefore, to accommodate misalignment during deployment, a strut must be twisted and bent, which introduces internal loads into the members. These loads are calculated and analyzed in the following sections.

#### 3.3.1 Longeron Strain and Moment

The longeron consists of a continuous member having a hinge fitting on each end of a graphite/epoxy tube of approximately one-meter length. At some degree of partial deployment, the relative orientations of the hinge axes on the two ends of the longeron are compared with their initial unstrained state, and any angular difference, which by symmetry is identical on the two ends, is resolved into the twisting and bending angles,  $\phi_{t_l}$  and  $\phi_{b_l}$ . See Figure 8.

Twisting each end through the angle  $\phi_{t_l}$  causes strain

$$\epsilon_{t_l} = \frac{\phi_{t_l} r_l}{l/2} \quad (\text{Reference 2, page 287})$$

where  $r_l$  is the longeron cross section outer radius. The generated torsional moment is

$$M_{t_l} = \frac{\phi_{t_l} GK_l}{l/2} \quad (\text{Reference 2, page 287})$$

Bending at each end, although not both in the same axial direction, can be modeled as such. Bending each end through the angle  $\phi_{b_l}$  produces a bow radius of  $R_l$  in the longeron given by

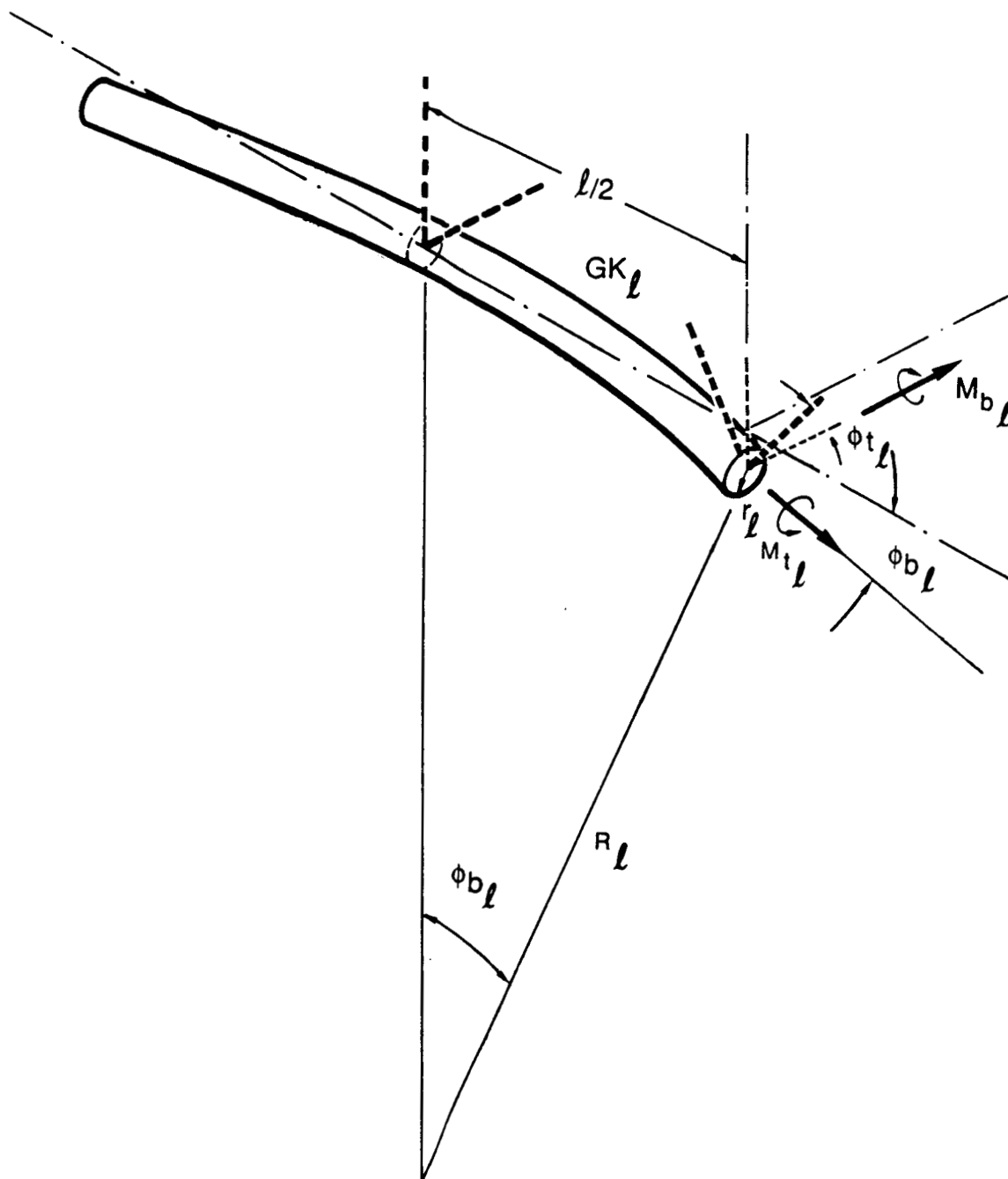


Figure 8. Longeron twisting and bending strain.



$$\frac{\ell/2}{R_\ell} = \phi_{b_\ell}$$

Strain and moment are then

$$\epsilon_{b_\ell} = \frac{r_\ell}{R_\ell} = \frac{2\phi_{b_\ell} r_\ell}{\ell}$$

$$M_{b_\ell} = \frac{EI_\ell}{R_\ell} = \frac{2\phi_{b_\ell} EI_\ell}{\ell}$$

Longeron strain and moment, for the point design, are plotted as a function of longeron angle in Figure 9.

### 3.3.2 Diagonal Strain and Moment

The diagonal is a non-continuous member, having a midspan hinge, two segments of graphite/epoxy tube, and a hinge fitting on each end, for an approximate total length of 1.6 meters. Figure 10 shows how the diagonal is analyzed during deployment. In (a), a single bay is shown fully packaged, with only one longeron and one complete diagonal visible for clarity. The partial deployment angle  $\theta_\ell$  is chosen, indicating the angle of the longeron away from vertical (beam axis), and in (b) the single bay is deployed to that condition, except the folded diagonal remains in its original position. The chord  $d_{AB}$  is determined, which is the required diagonal end-end length. In (c) the diagonal is unfolded about its midspan hinge, duplicating the chord length  $d_{AB}$ . In (d) the two segments of the diagonal are rotated as a rigid body (no rotation about midspan hinge) about the base hinge at  $A_1$  so that the other end approaches corner body  $B_1$ . In (e) both ends of the diagonal are freed in rotation, but connected at corner bodies  $A_1$  and  $B_1$ , and the diagonal is rotated about axis  $A_1B_1$  to obtain minimum angular mismatch. This orientation is then fixed relative to the partially deployed bay, and in (f) the bay is oriented so that the base segment of the diagonal is along the x-axis and the hinge in corner body  $A_1$  is in the x-y plane. In (g) the region at corner body  $A_1$  is expanded, so that the required angles of twisting  $\phi_{t_d}$  and bending

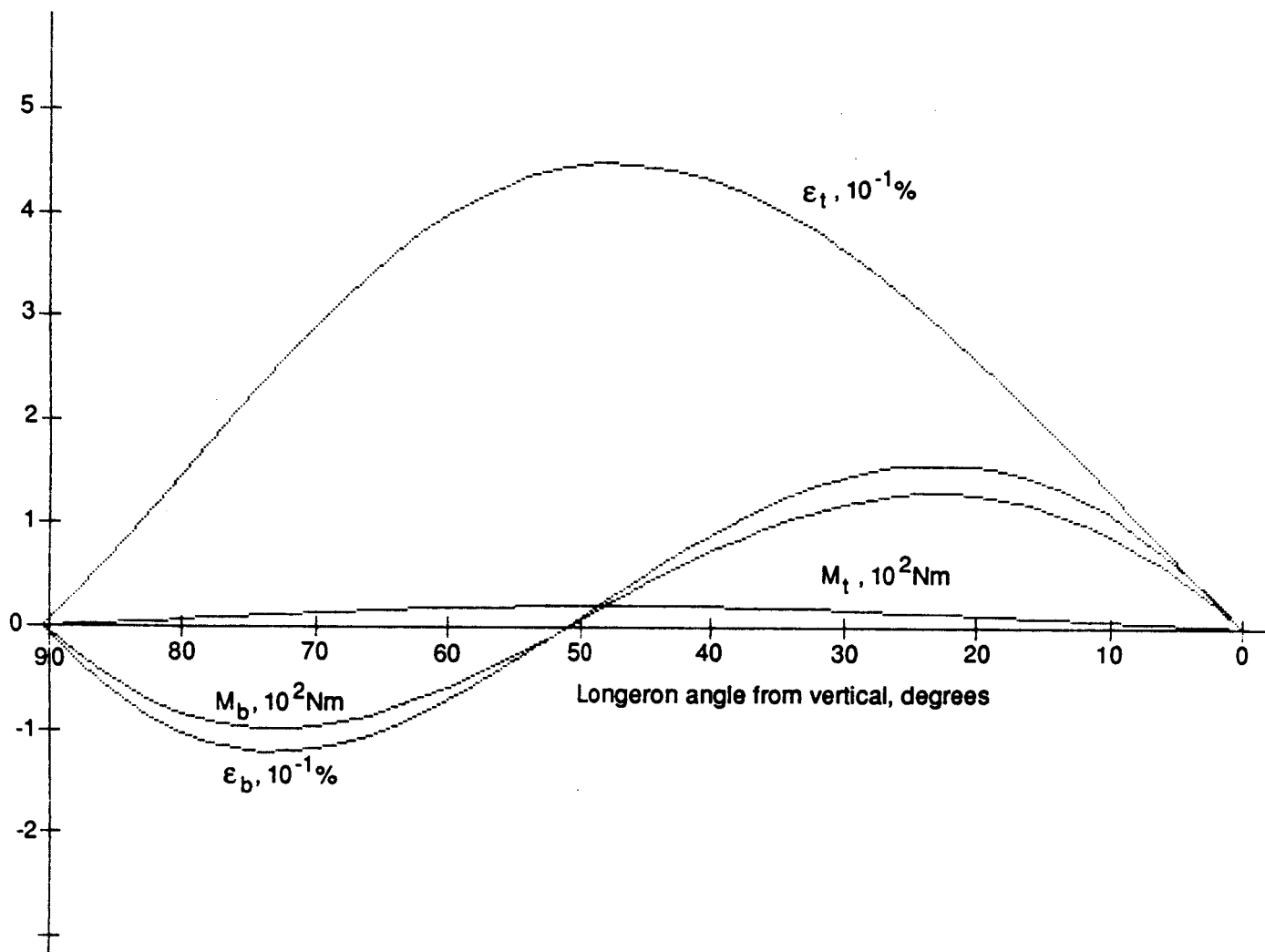


Figure 9. Longeron bending and twisting strains and moments.

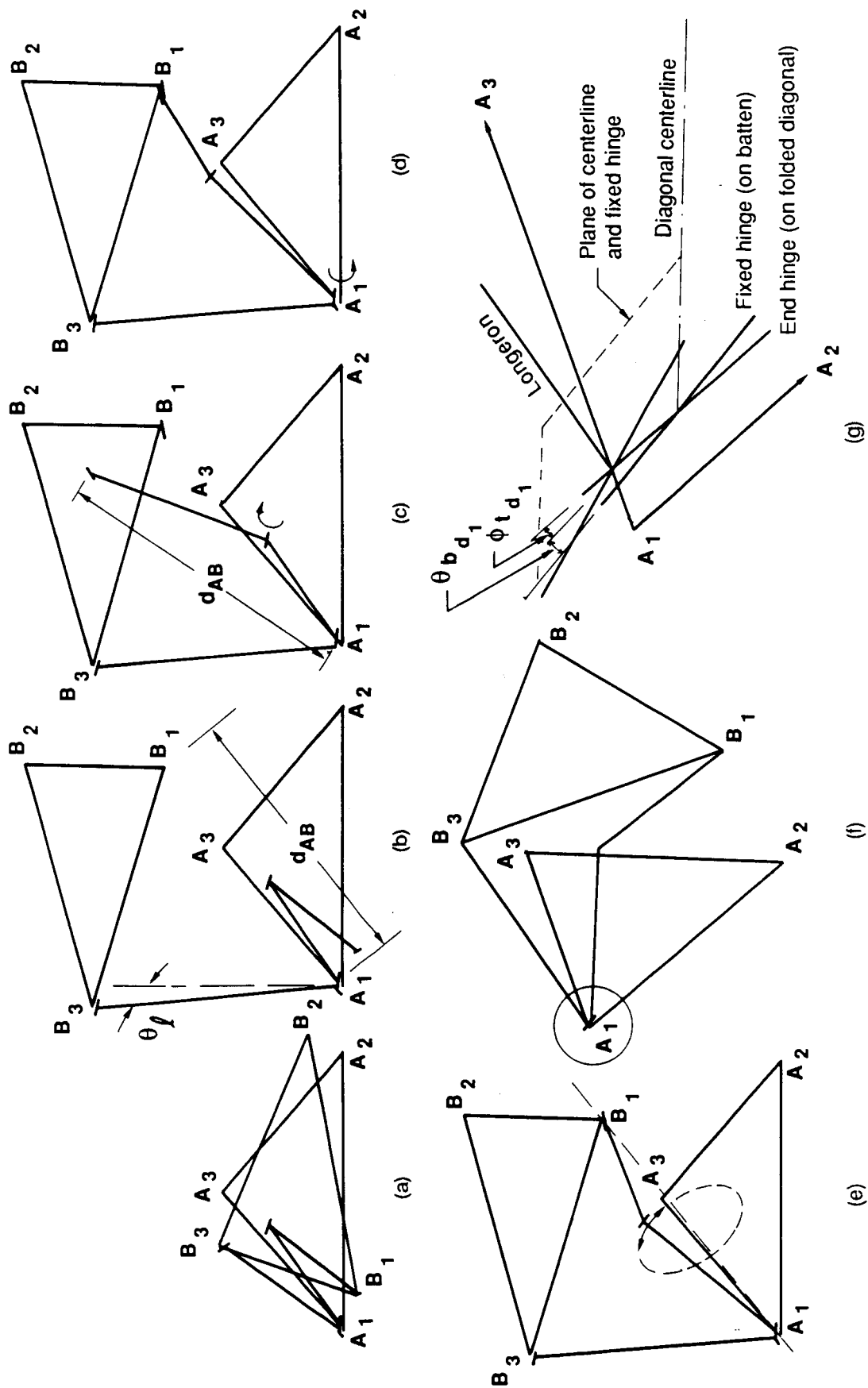


Figure 10. Diagonal strain determination.

$\phi_{bd}$  are clarified. Steps (f) and (g) are repeated for obtaining strains in the other segment of the diagonal. Diagonal strains and moments are then obtained as follows:

Twisting of the end through the angle  $\phi_{td}$  causes strain

$$\epsilon_{td} = \frac{\phi_{td} r_d}{d_n}$$

where  $r_d$  is the diagonal cross section outer radius and  $d_n$  is the diagonal segment length (end to midspan hinge). The generated torsional moment is

$$M_{td} = \frac{\phi_{td} GK_d}{d_n}$$

In determining the effect of bending at the end, it is assumed that, at the midspan hinge, the member is pinned. Then, the generated bending moment at the end is

$$M_{bd} = \frac{3EI_d \phi_{bd}}{d_n}$$

The bending radius is

$$R_d = \frac{EI_d}{M_{bd}} = \frac{d_n}{3\phi_{bd}}$$

so that the strain is

$$\epsilon_{bd} = \frac{r_d}{R_d} = \frac{3\phi_{bd} r_d}{d_n}$$

Diagonals 1 and 2 strain and moment, for the point design, are plotted as a function of longeron angle in Figures 11 and 12.

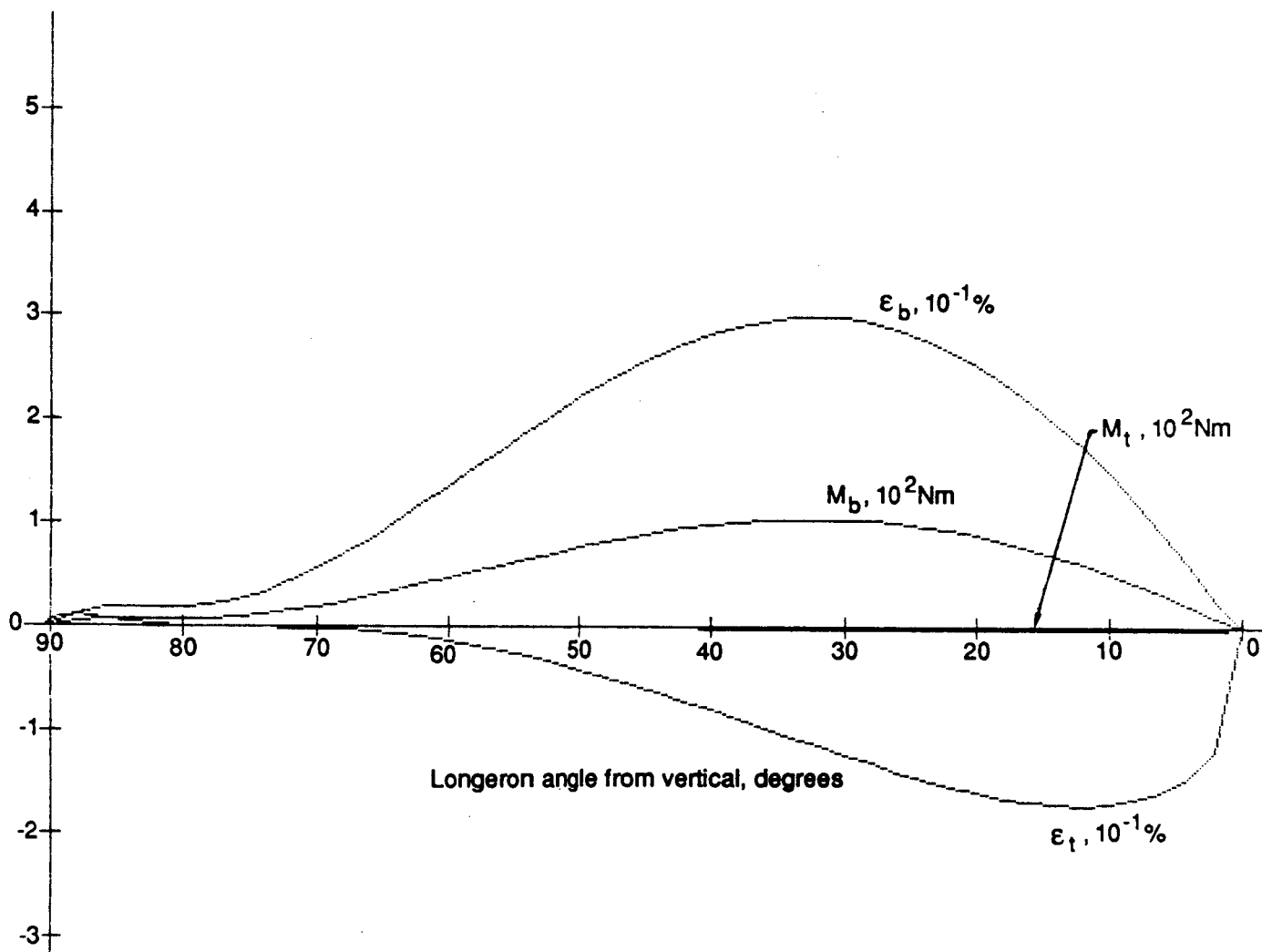


Figure 11. Diagonal 1 bending and twisting strains and moments.

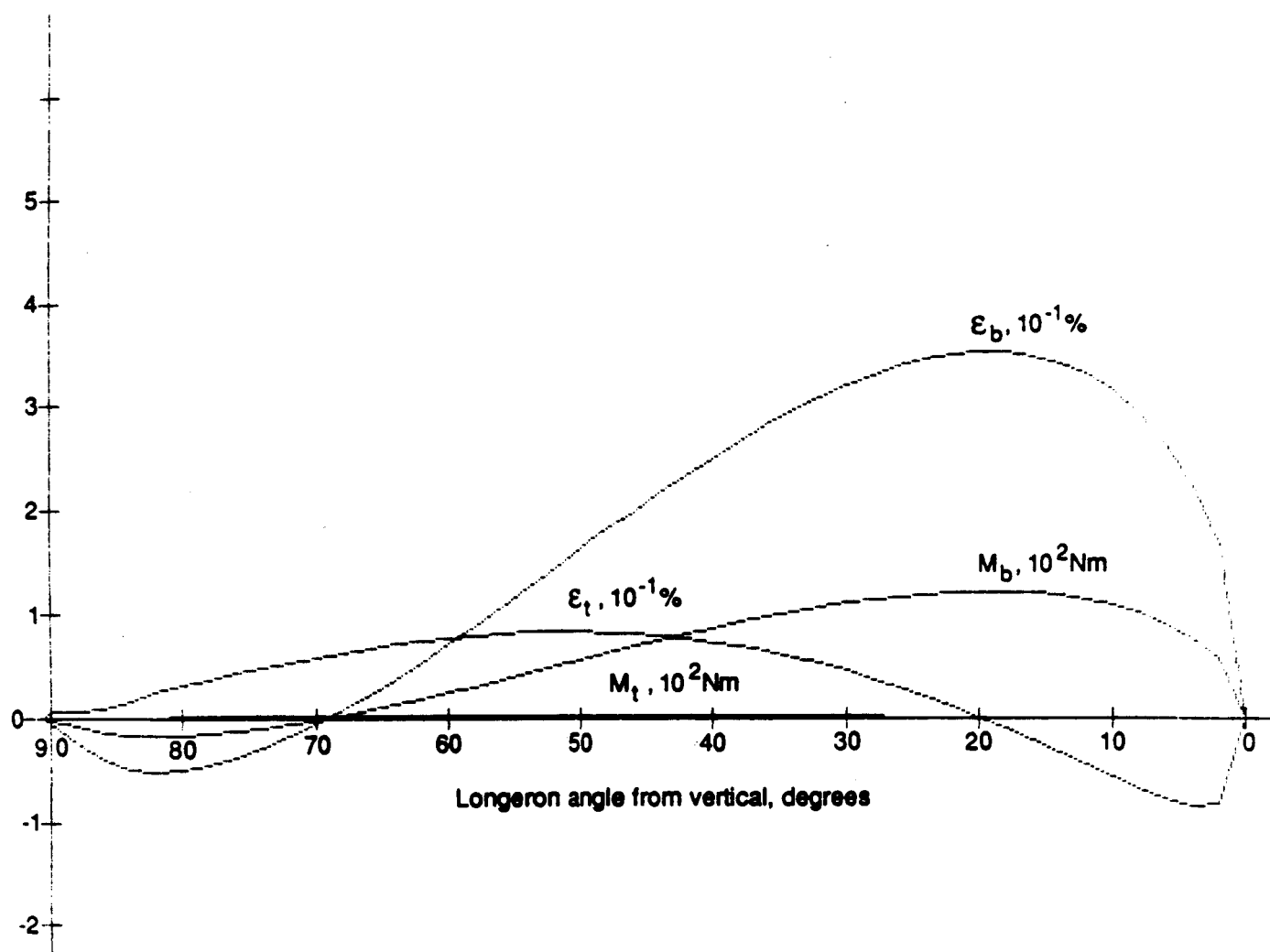


Figure 12. Diagonal 2 bending and twisting strains and moments.

### 3.3.3 Deployment Forces and Energy

Since work is required to twist and bend members, force must be applied over a distance to deploy or retract the beam. The change in flexural energy in any member in twisting or bending is

$$\Delta E = M \Delta \phi$$

where M is the instantaneous generated moment and  $\Delta \phi$  is the angle, in radians, through which the moment applies. Beam energy changes as the sum of the member energies. Since there are six longeron ends and three of each diagonal end per bay,

$$\begin{aligned} \Delta E_{\text{bay}} = & 6(M_{t_{\ell}} \Delta \phi_{t_{\ell}} + M_{b_{\ell}} \Delta \phi_{b_{\ell}}) + 3(M_{t_{d_1}} \Delta \phi_{t_{d_1}} + M_{b_{d_1}} \Delta \phi_{b_{d_1}}) \\ & + 3(M_{t_{d_2}} \Delta \phi_{t_{d_2}} + M_{b_{d_2}} \Delta \phi_{b_{d_2}}) \end{aligned}$$

Then, as the bay deploys, the total flexural energy of the bay is

$$E_{\text{bay}} = \Sigma \Delta E_{\text{bay}}$$

Deployment forces are determined assuming that the beam energy is the product of the force exerted along a certain direction and the distance moved in that direction. Axial deployment force is

$$F_a = \frac{\Delta E_{\text{bay}}}{\Delta z}$$

where z is the instantaneous height of the moving "B" batten frame. Radial deployment force (exerted on diagonal midhinges) is

$$F_r = \frac{\Delta E_{\text{bay}}}{\Delta s}$$

where s is the instantaneous diagonal midhinge displacement.

Figure 13 shows single-bay energy and forces. Positive forces retard deployment; negative forces push toward full deployment or, conversely, retard retraction. Starting from the fully packaged state on the left side of the graph, axial deployment load increases because of longeron bending strain (Figure 9). The longerons then straighten out, so that deployment load decreases and actually pushes toward full deployment. Longeron bending then increases, but in the opposite direction, while concurrently diagonal bending is becoming significant, and deployment load approaches 100 N (22 lbf). During the final stage of deployment, strut members straighten out as bay height approaches the fully deployed bay length, and axial deployment force becomes highly negative. Although member twisting strain is significant, the torsional stiffness of the unidirectional graphite/epoxy tubes is so low that member torque does not greatly affect deployment load.

At full deployment (right side of graph, Figure 13), the changing strain energy of the single bay can be expressed as the work done in retracting the bay by pushing on the diagonal midspan hinges. This force reaches a peak of about 140 N (31 lbf). At a longeron angle of about 15 degrees from the axial direction during retraction, the axial deployment force becomes manageable so that forces pushing on diagonal midspan hinges can be replaced by forces pushing axially downward (toward retraction).

### 3.4 HINGE DESIGN AND TEST STUDIES

As indicated in Section 3.1.1.1, hinge compliance is a very important factor in beam design. The joint stiffness "knockdown" factor can be significant in designs where the longeron strut is axially very stiff. In the present design the longeron stiffness  $EA_L$  is about  $17 \times 10^6$  N ( $3.8 \times 10^6$  lbf), so that over its 1.12-meter (44-inch) length, it has a compliance of 66 nm/n (11.5  $\mu$ in/lbf). A knockdown factor of two-thirds implies a compliance increase of 50 percent, or 33 nm/N (5.8  $\mu$ in/lbf) for the sum of the two longeron end fittings. As shown in the following sections, this compliance is easily achievable.



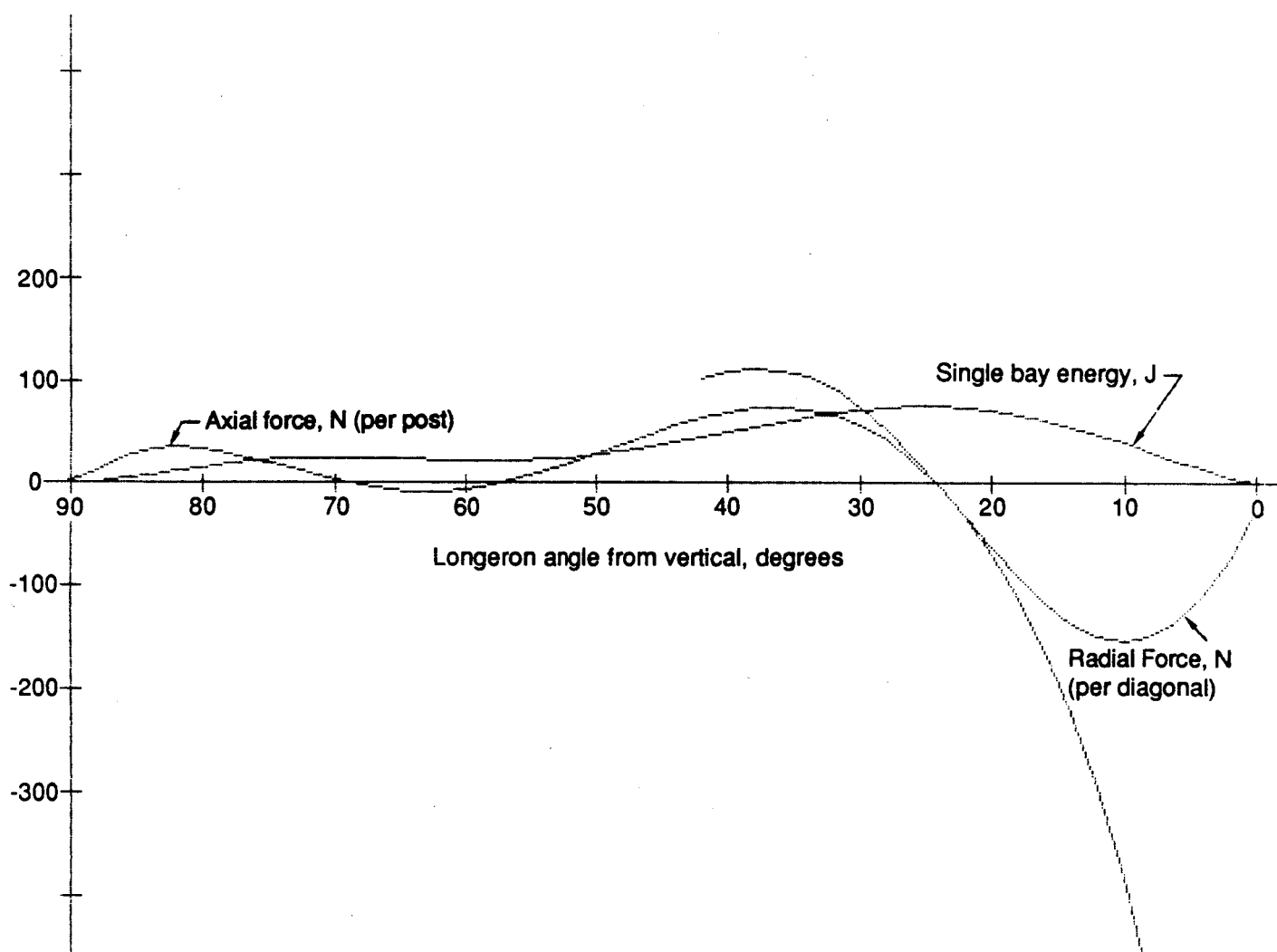


Figure 13. Forces and energy.

### 3.4.1 Hinge Design

Hinges in most cases of the present design are designed to be simple clevises, so that the ends of the longerons and diagonals consist of a single tang with a hole, fitting into slots in the corner bodies which also have holes. Hole directions are as given in Table 1, and slots are perpendicular to holes. Diagonal midspan hinges are a special case, and are discussed in Section 3.4.3.

### 3.4.2 Test

Two effects which are observable in hinge tests are of significant importance in deployable trusses: compliance and turning moment. As discussed in Section 3.1, hinge fitting compliance, measured as fitting deflection per unit of force applied in the direction of a member centerline, determines along with strut axial stiffness the axial and bending stiffnesses of the beam. The moment required to turn a strut about its hinge axis affects the deployability of the beam. Beams of large cross section, having long struts, can tolerate greater hinge turning moment than can smaller beams. The deployment load, discussed in Section 3.3, is affected by this moment, as work is required in rotating these hinges. Compliance is separable into the three areas of elastic deformation, hysteresis, and deadband. Turning moment is a function of pin-to-hole clearance and friction coefficient.

Tests were conducted on a number of configurations using the apparatus shown in Figure 14 to determine the shape of the force deflection curve, and in so doing find design approaches which maximize joint stiffness while minimizing hysteresis and deadband.

Figure 15 shows the performance progression during a series of hinge compliance tests, showing the necessity for very close precision fits between pin and hole as well as tang width and slot width, and for hard, low-friction coatings. A typical compliance test (Figure 15a) displays all three compliance characteristics: deadband as an abrupt change in slope near zero load as the part clearances adjust for load direction; hysteresis as a broadening of the curve due to load transfer effects across pin-lug boundaries; and elastic deformation of the material itself, seen as a constant slope in regions away

ORIGINAL PAGE IS  
OF POOR QUALITY

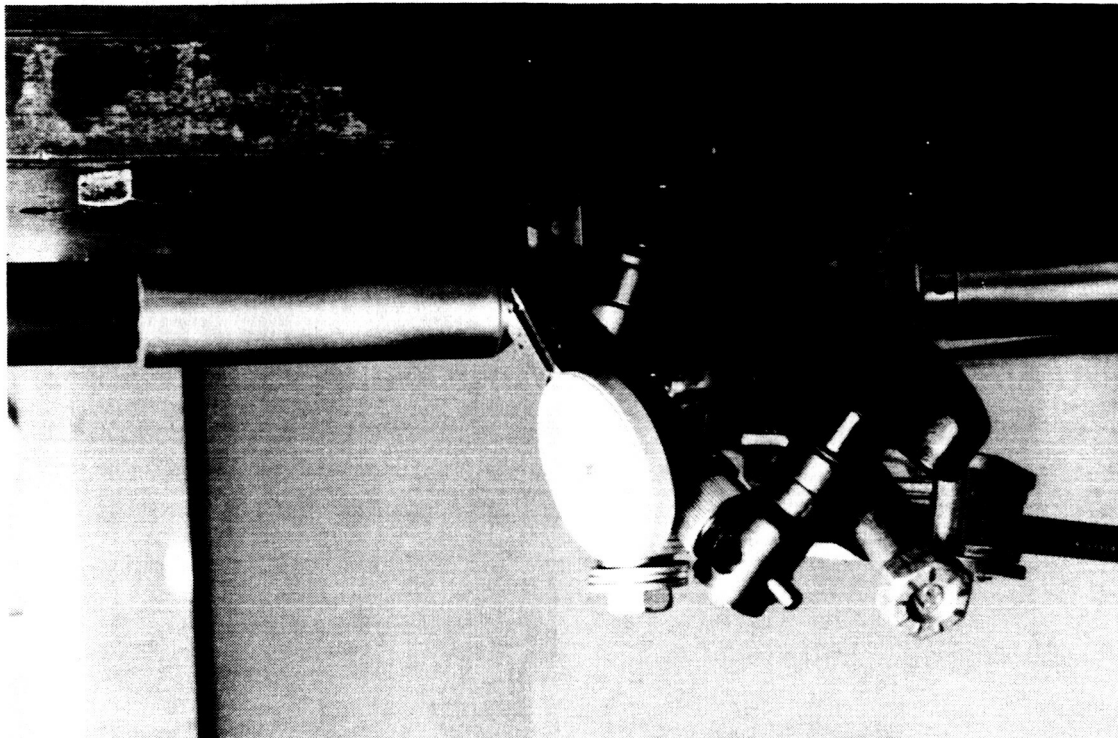


Figure 14. Longeron compliance test.

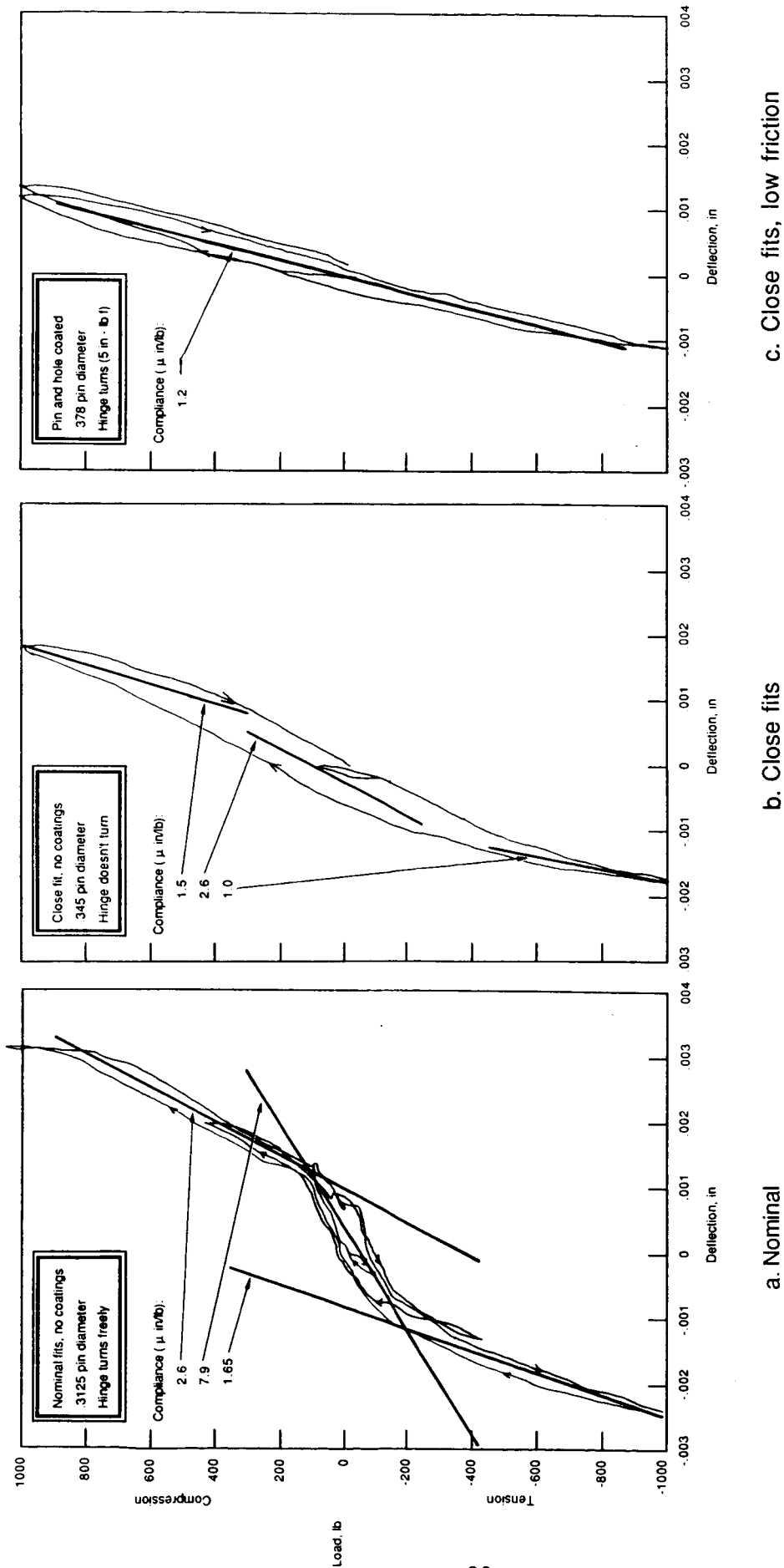


Figure 15. Compliance test results showing necessity for close fits and low friction.

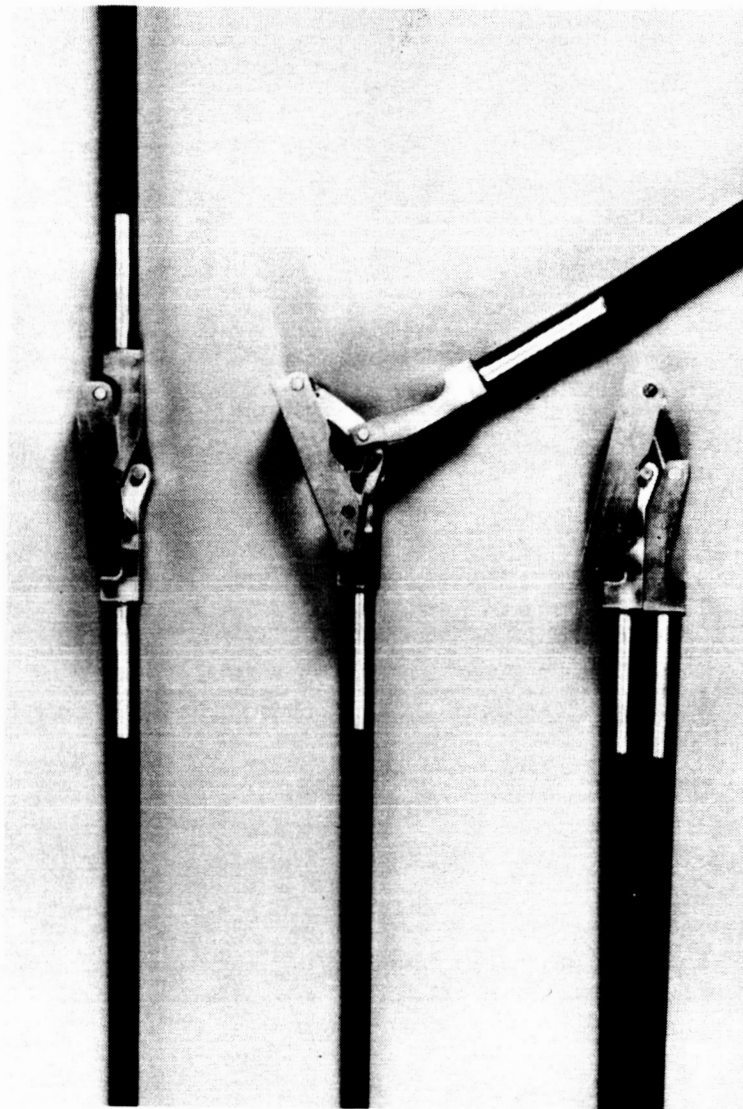
from zero load. Early efforts were directed toward minimization of deadband by using very close fits, and in Figure 15b, the deadband is nearly eliminated (measured diametral clearance: 0.00015 inch, each of two pins). This part refused to turn, in spite of the measured clearance. In Figure 15c, coated pins were used (Nedox CR+), with similar clearance as before, and compliance was satisfactorily low, as was the turning moment. Throughout the test series, successively increasing pin diameters were used (from 0.315 inch at start to 0.378 inch at end of series), with no noticeable decrease in compliance due to this effect. It was concluded that hard, low-friction coatings are necessary, with very close fits, yielding hinge compliances of less than 5.7 nm/N (1.0  $\mu$ in/lbf) and hinge turning moments of less than 0.56 Nm (5 in-lbf).

### 3.4.3 Diagonal Midspan Hinges

Preloading hinges are used as diagonal midspan hinges. This concept has been used in several deployable structures (References 3, 4, 5 and 6), resulting in the development of a highly efficient hinge. General requirements include:

- High preload in deployed condition in terms of bending moment and compressive load across contact face.
- Relatively high bending moment tending toward full deployment as fold angle approaches zero.
- Low compliance

The geometric properties of the hinge, which consists of an assembly of two main bodies and two links, amplify the moment applied by a torsion spring several times to generate the deployed preload. In Figure 16a, the spring is in the long link, where it attaches to the body. High moment amplification results because the links approach parallelism in the deployed condition. Note that the pictorial perspective disguises the fact that the fully packaged hinge folds to an included angle of about 14 degrees, as shown in Figure 5. The linkage schematic (Figure 16b) indicates how moment amplification is related to hinge geometry. At full deployment, moment amplification is quite high if the link-link angle  $\alpha$  is low, and if the link stand-off distance  $l_{bd}$  is large.

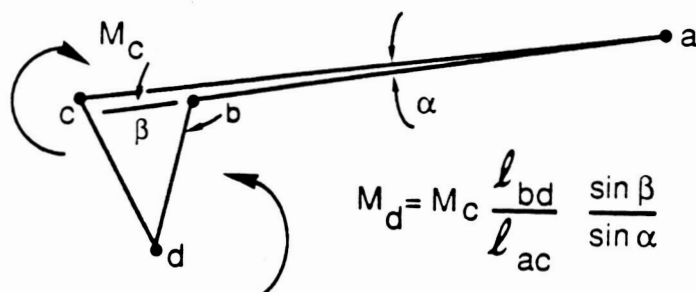


Deployed

Partially  
deployed

Stowed

a. Truss beam model hinge.



b. Schematic

Figure 16. Diagonal hinge.

## SECTION 4

### TRUSS BEAM DESIGN, FABRICATION AND ASSEMBLY

#### 4.1 MATERIALS

Materials used in the various components of this assembly include:

- Longerons: Graphite/epoxy tube, unidirectional axial filaments, material type Celanese G50. Glass scrim used mid-wall to increase circumferential strength. Outer diameter measured 0.02012 meter (0.792 inch), wall measured 0.00257 meter (0.101 inch).
- Diagonals: Graphite/epoxy tube, unidirectional axial filaments, material type Celanese G50. Glass scrim used mid-wall to increase circumferential strength. Outer diameter measured 0.01504 meter (0.592 inch), wall measured 0.00191 meter (0.075 inch).
- Battens: Graphite/epoxy tube, unidirectional axial filaments, material type Celanese G50. Glass scrim used mid-wall to increase circumferential strength. Outer diameter measured 0.01496 meter (0.589 inch), wall measured 0.00146 meter (0.058 inch).
- Hinge fittings: All fittings and corner bodies were machined titanium alloy Ti-6Al-4V. Surfaces were coated, including clevis sides and holes and excluding bonding surfaces, using Tiodize 2X, which is a proprietary titanium surface coating. Coating thickness was 20 to 50 microinches.
- Hinge pins: 303 stainless steel, drilled and tapped for retrieval. Pin surfaces were coated using Tiolube 1175, a proprietary titanium surface coating. It is essentially a molybdenum disulfide formulation, 0.001 to 0.002 inch thick.

#### 4.2 FIXTURES

Fixturing was designed and fabricated for bonding components together, which consisted of bonding hinge fittings to graphite/epoxy tubes. Hinge pin spacing and orientation were of equal importance, and were held close to tolerance by the use of tooling balls and accurate ramp angles and distance measurements, and by the use of the same fixture for many bonding operations.

Since all batten frames are triangular with a 0.7-meter radius, the same fixture was used for bonding of all "A" and "B" batten frames, as shown in

Figure 17. For placement of each corner body, a simulated longeron fitting was inserted in an accurately located hole, and each was clamped in the proper orientation.

Longerons are of two types, which are identical in length but are mirror images of each other. Hence, the same fixture was used for all, and left- and right-handed fitting orientations were accomplished by the use of invertible ramps. Figure 18 shows the method for longeron bonding.

Diagonals consist of midspan hinges, graphite/epoxy tubes, and end fittings. Bonding of diagonals was done in two steps: first the graphite/epoxy tubes were bonded to the midspan hinge in the deployed configuration, and then the end fittings were bonded in place. The first step was done independently to ensure colinearity of deployed diagonal segments. Since, as with the longerons, there are two types of diagonals, identical in length but mirror images of each other, the same fixture was used for all diagonals, using invertible ramps for opposites. Figure 19 shows the method for bonding midspan hinges; the bonding method for the diagonal end fitting is the same as shown for the longerons in Figure 18.

#### 4.3 BONDING PROCEDURES

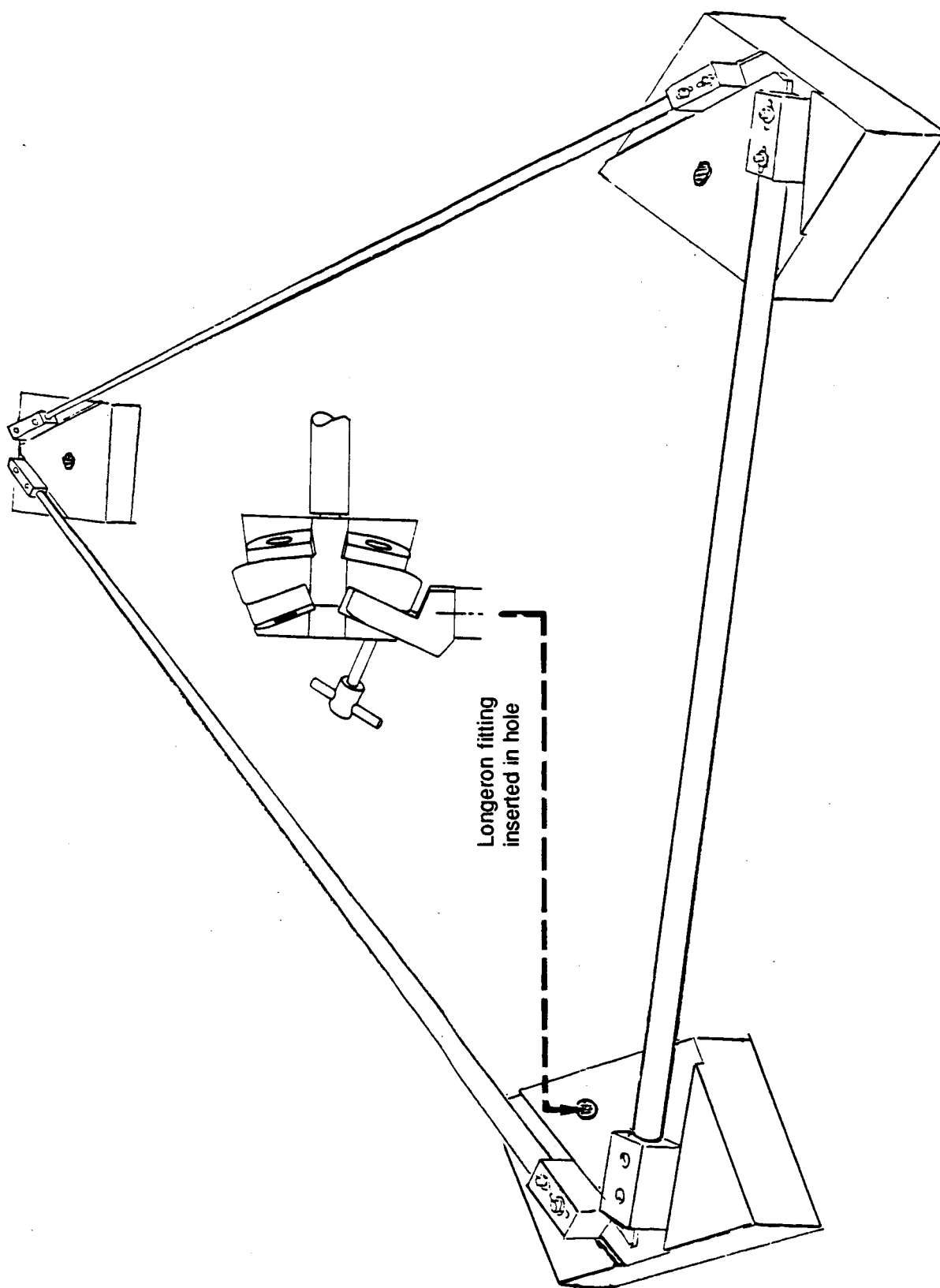
Procedures used for bonding the truss beam piece parts together were similar to those developed for the Seasat radar antenna deployable beam fabricated at Astro Aerospace Corporation from titanium and graphite/epoxy. Titanium was pretreated using Passajel 107. Graphite/epoxy tube ends were pretreated by abrasion using 120 grit sandpaper, followed by immersion in Silane. Epoxy adhesive 934 NA was used, with a two-hour cure at 40°C.

#### 4.4 TESTS

##### 4.4.1 Tube Acceptance Tests

Acceptance tests of the graphite/epoxy tubes were performed to confirm that they were of required stiffness. Two types of test were conducted: three-point bending and free-free vibration. In the first, the tube is





Longeron fitting  
inserted in hole

Figure 17. Batten bonding fixture.

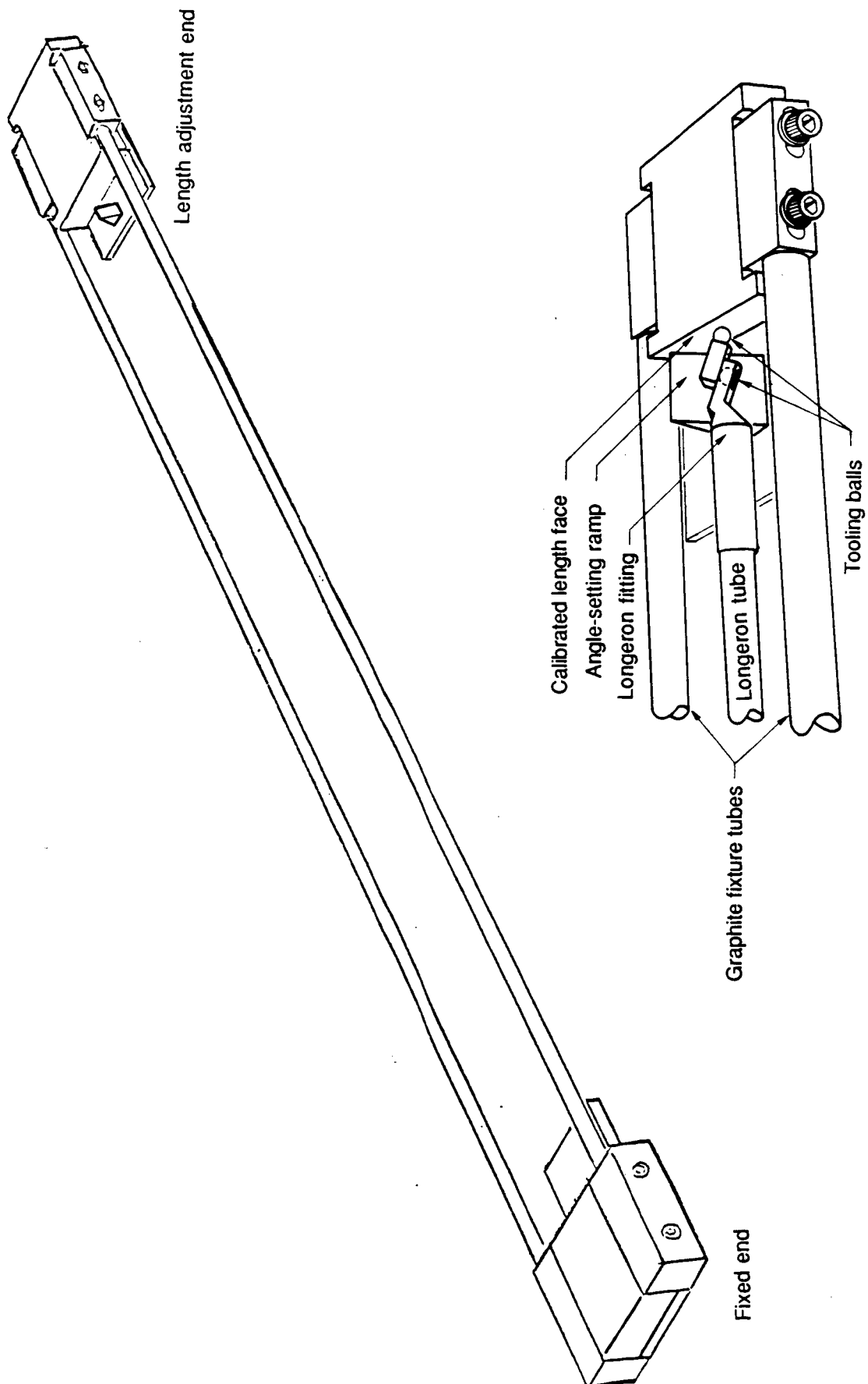


Figure 18. Longeron bonding fixture.

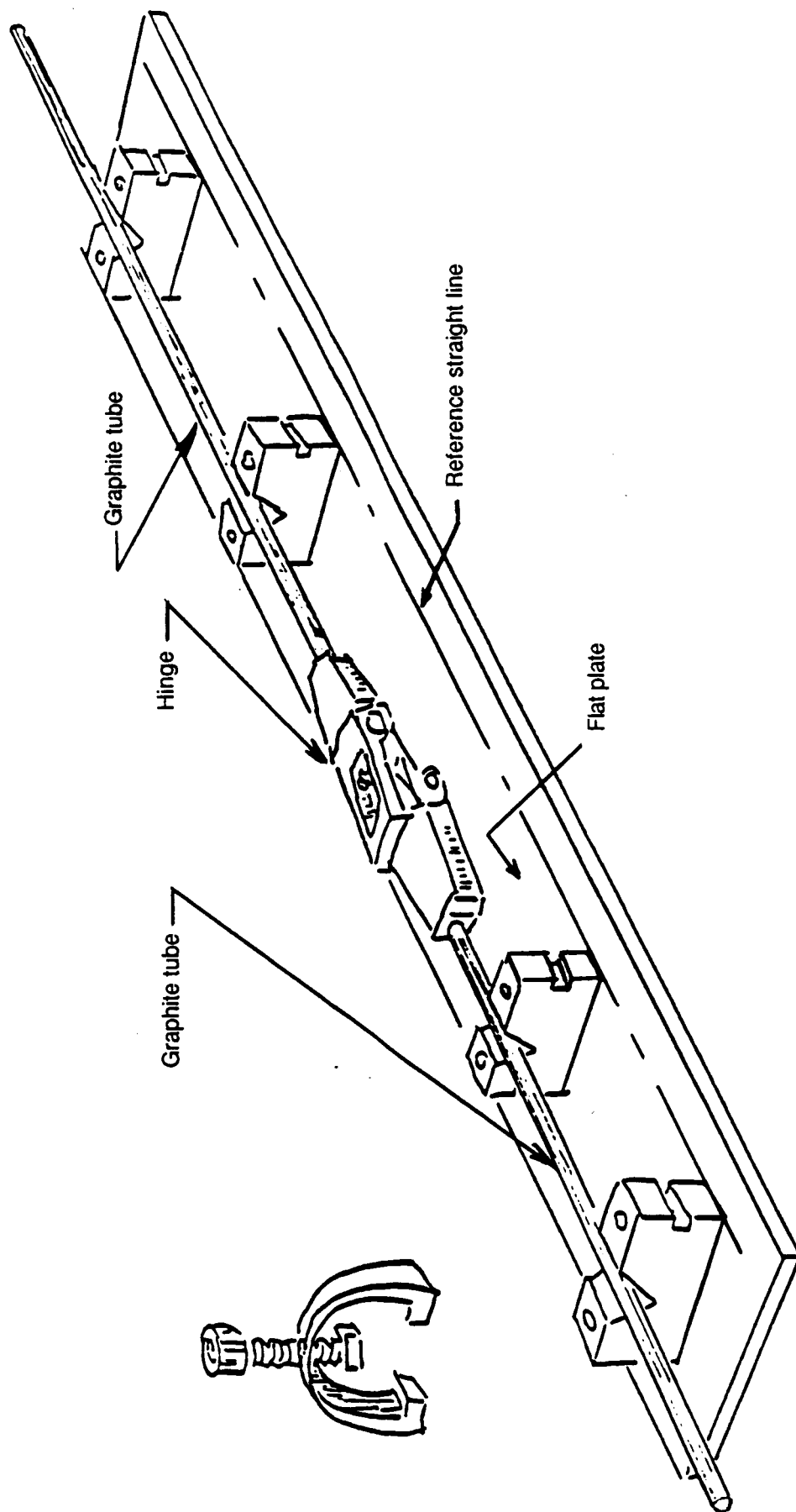


Figure 19. Diagonal hinge and tube alignment.

supported horizontally at two points separated by distance  $l$ , and load  $P$  is applied vertically to the tube at the midpoint between the supports. The deflection  $y$  is

$$y = - \frac{Pl^3}{48EI} \quad (\text{Reference 2, Table 3, case 1e})$$

The areal moment  $I$  is obtained from the tube cross section (Section 3.1.1.2), so that the tube modulus  $E$  is determined from the slope  $P/y$  of the load-deflection curve.

The second method of determining tube modulus, by free-free vibration, consists of supporting the tube vertically (hand-held is satisfactory) at a distance of 0.224 times its total length from its upper end, which is a nodal point for this vibration. The tube is struck at its center and the resulting tone identified by comparison to standard tones. The frequency is

$$f = \frac{22.4}{2\pi} \sqrt{\frac{EI}{m'l^3}} \quad (\text{Reference 2, Table 36, case 4})$$

The lineal mass  $m'$  is measured directly on an accurate balance; areal moment  $I$  is obtained as previously. Then the tube modulus is determined from the measured frequency as listed in a standard tone-frequency chart. Supporting the tube at nodal points corresponding to higher harmonics and using the appropriate constant (Reference 2, Table 36, case 4) yields corroborative data.

The two methods yielded modulus results typically within five percent of each other, with the acoustic result generally being higher.

#### 4.4.2 Member Proof Tests

Proof tests were conducted on members for two reasons. First, early in the development period to aid in the design of end fittings, bending and twisting moments were applied at the bond area between the tube and fitting at the predicted deployment load level, and after a series of tests a fitting design was developed in which tube loadings are transferred into the fitting through an internal stub and an external sleeve. The second stage of member

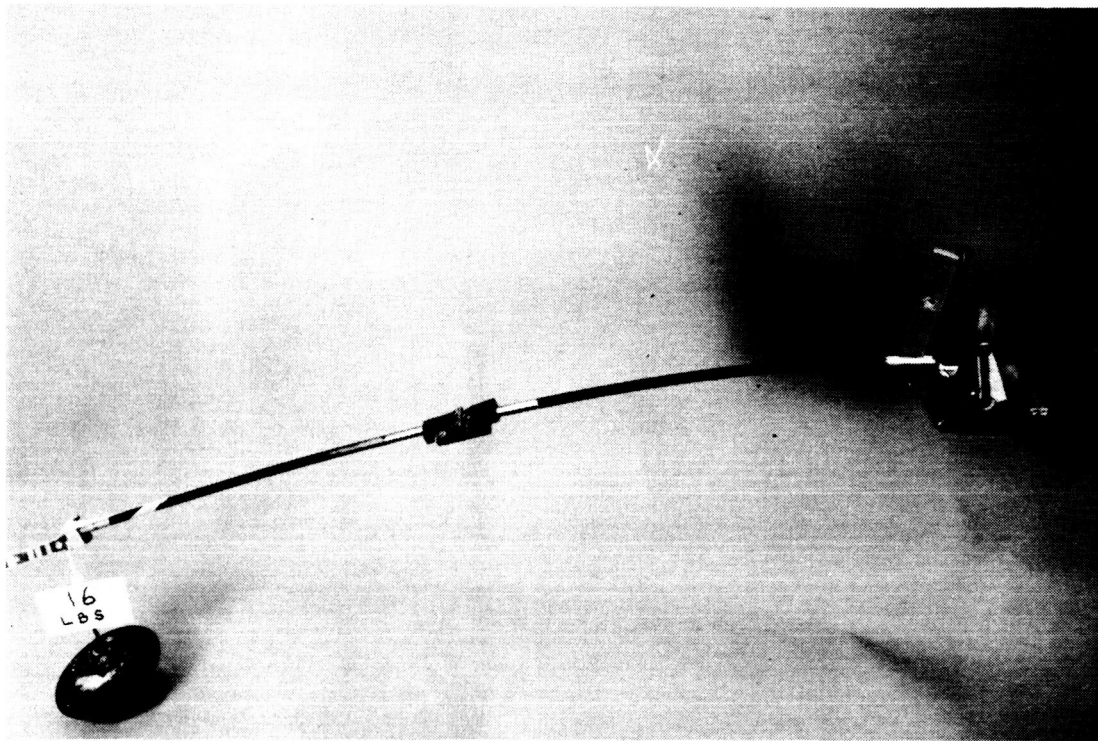
proof tests served to qualify the graphite/epoxy tube in each member for bending and twisting at the deployment load level. Figure 20 shows these tests as they were conducted. Twisting strain was developed over the entire tube length; bending strain was maximum at the support point. These proof tests were conducted in a quiet environment, and any audible cracking noises were grounds for rejection of a part. Other inspection techniques could have been used here (x-ray, acoustic emission, etc.), but this procedure was selected to keep inspection costs low.

#### 4.5 ASSEMBLY

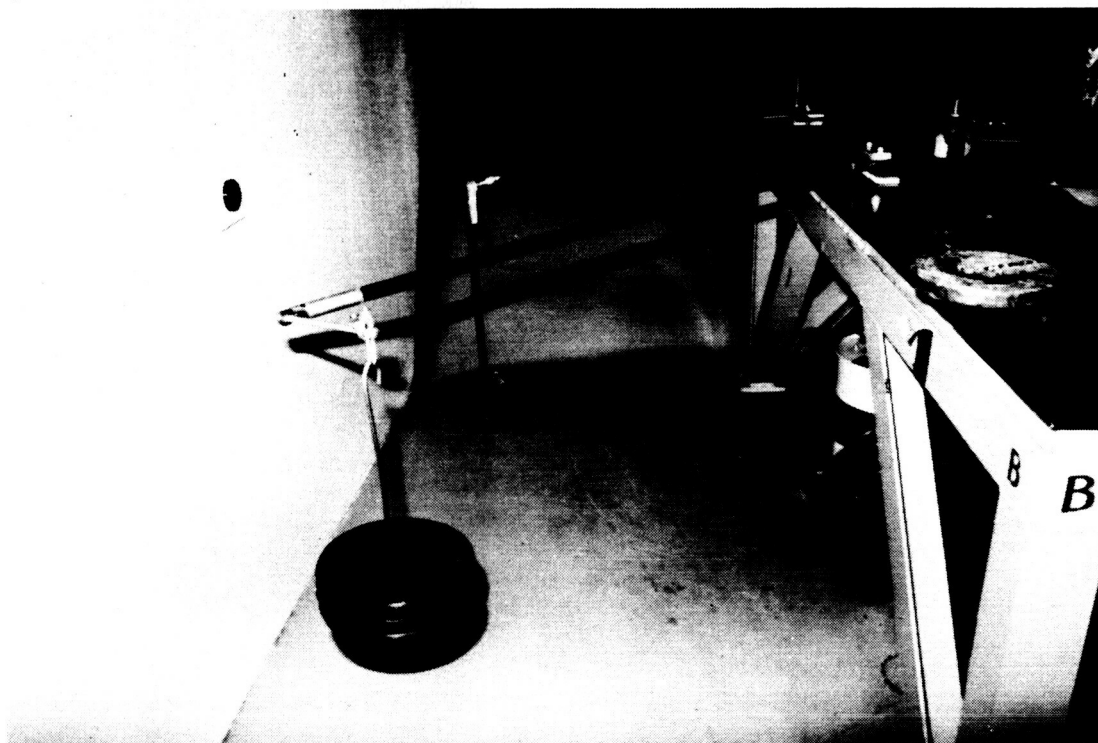
Beam subassemblies are shown in Figure 21 and consisted of longerons and diagonals, both in left- and righthanded versions, and A- and B-type batten frames.

Beam assembly consisted of pin insertion. Pins were cooled by immersion in liquid nitrogen, so that a diametral clearance of about 0.0003 inch was achieved during pin insertion. At temperature equilibrium, the pin-hole clearance is nominally zero. Care was taken to assemble components properly, as pin removal is difficult (but possible). Figure 22 shows the assembled beam in the packaged state. Figure 23 shows partial deployment. In Figure 24 the beam is fully deployed.

ORIGINAL PAGE IS  
OF POOR QUALITY



b) Diagonal



a) Longeron

Figure 20. Member proof tests.

ORIGINAL PAGE IS  
OF POOR QUALITY

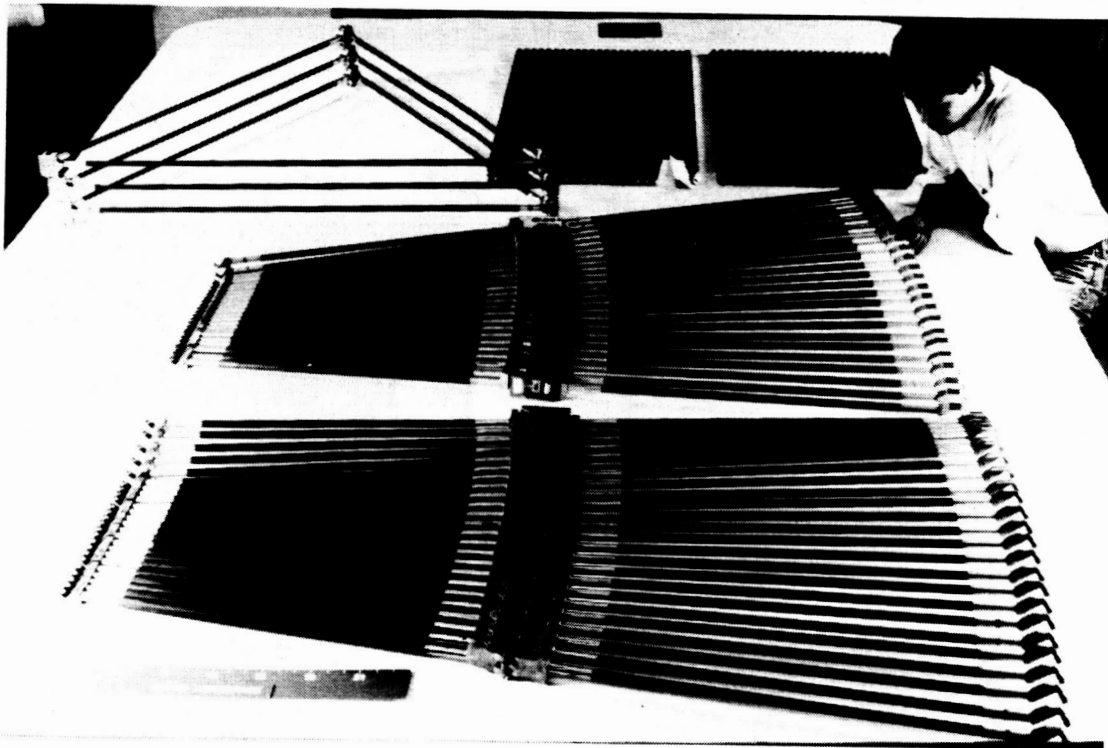


Figure 21. Preassembled beam parts.

ORIGINAL PAGE IS  
OF POOR QUALITY

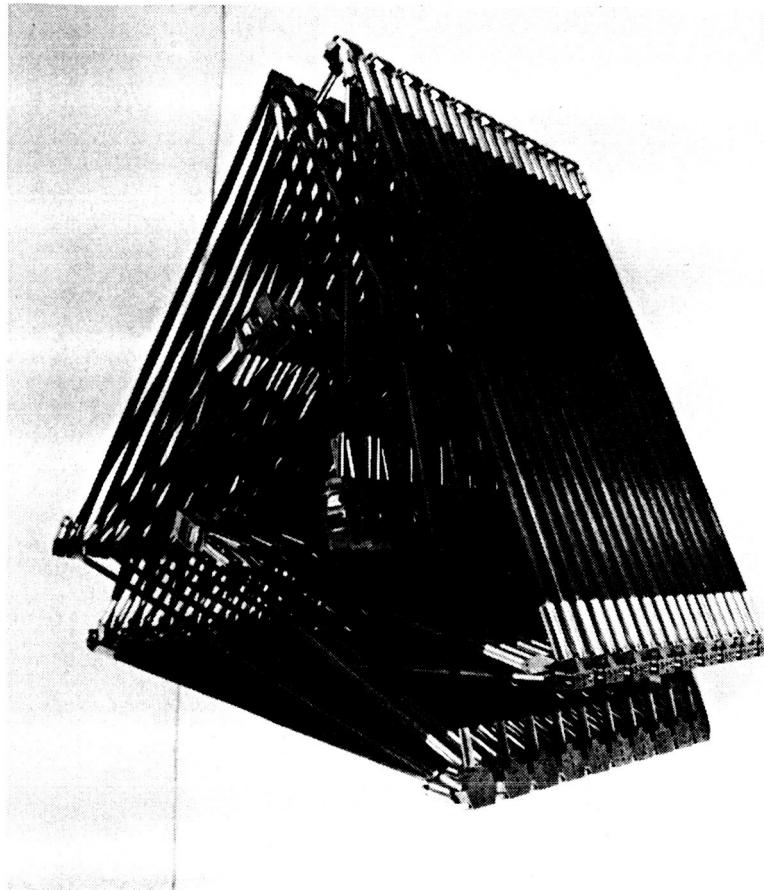
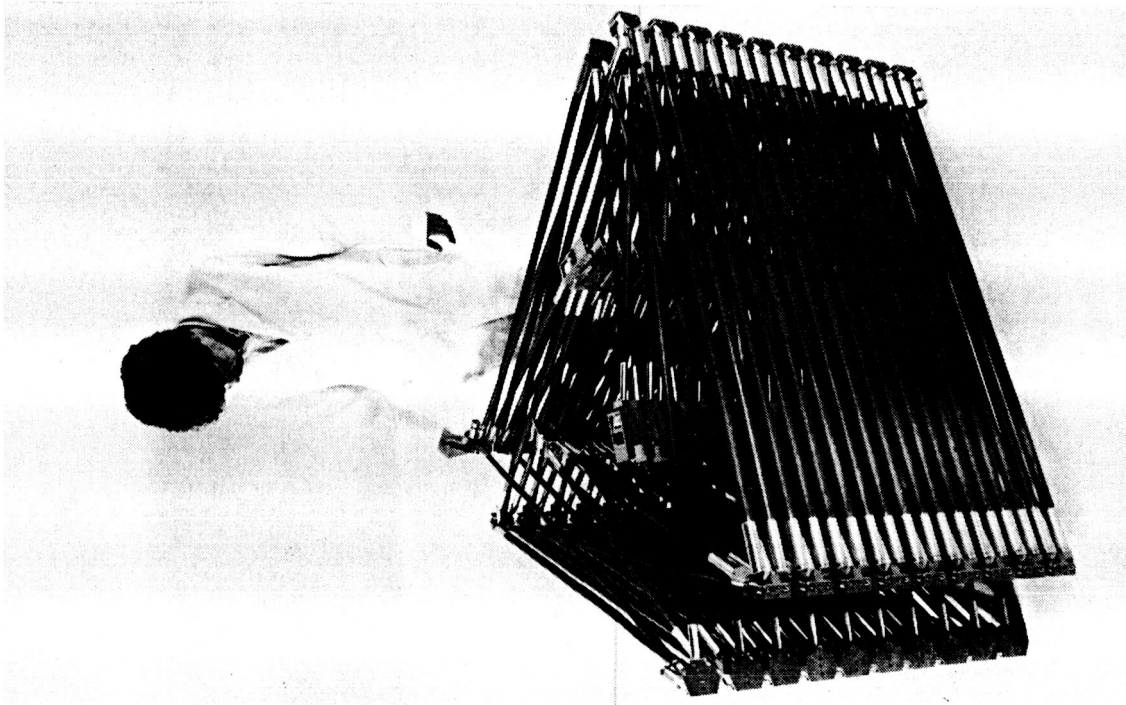


Figure 22. Assembled beam, packaged.



ORIGINAL PAGE IS  
OF POOR QUALITY

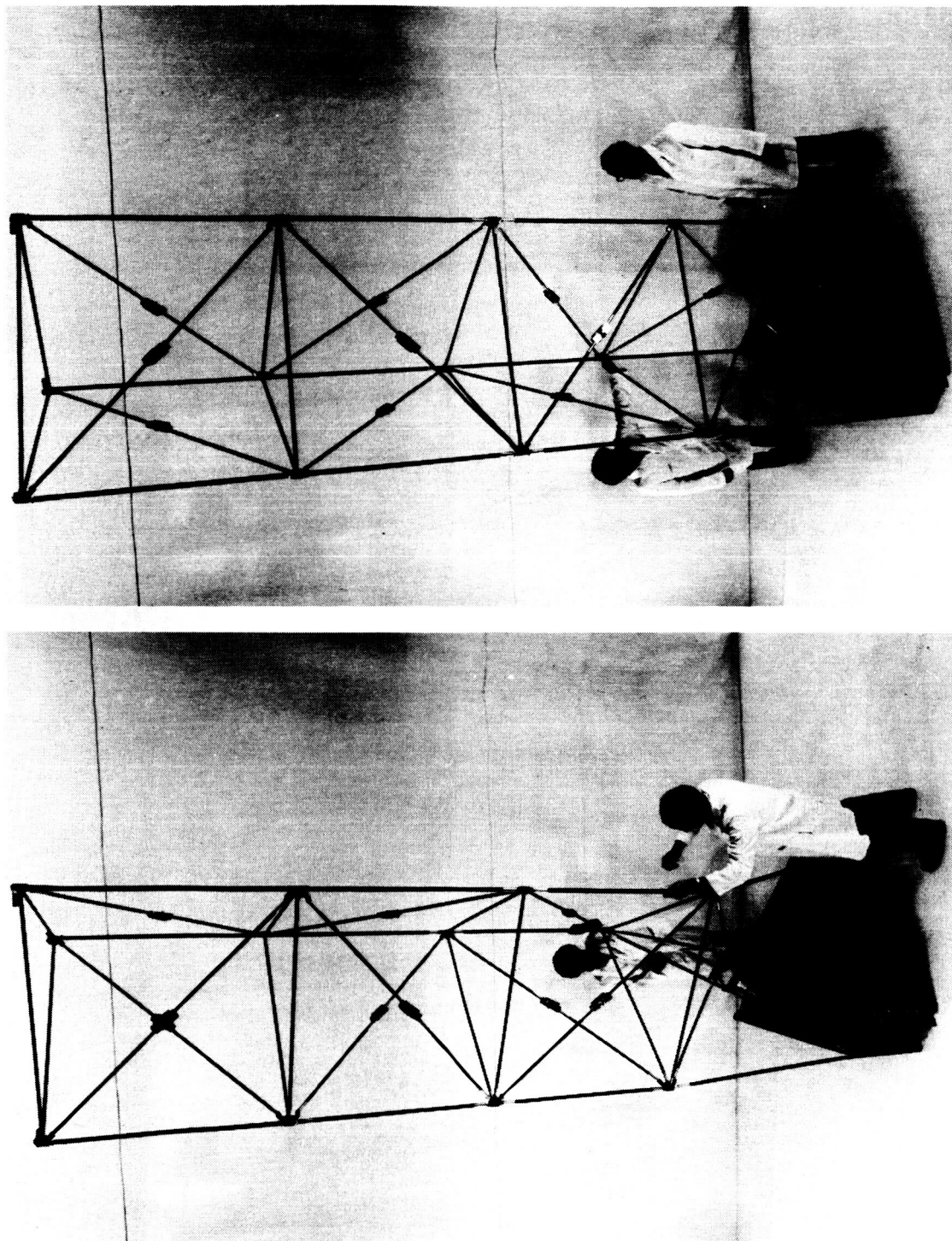


Figure 23. Partial deployment of assembled beam.

ORIGINAL PAGE IS  
OF POOR QUALITY

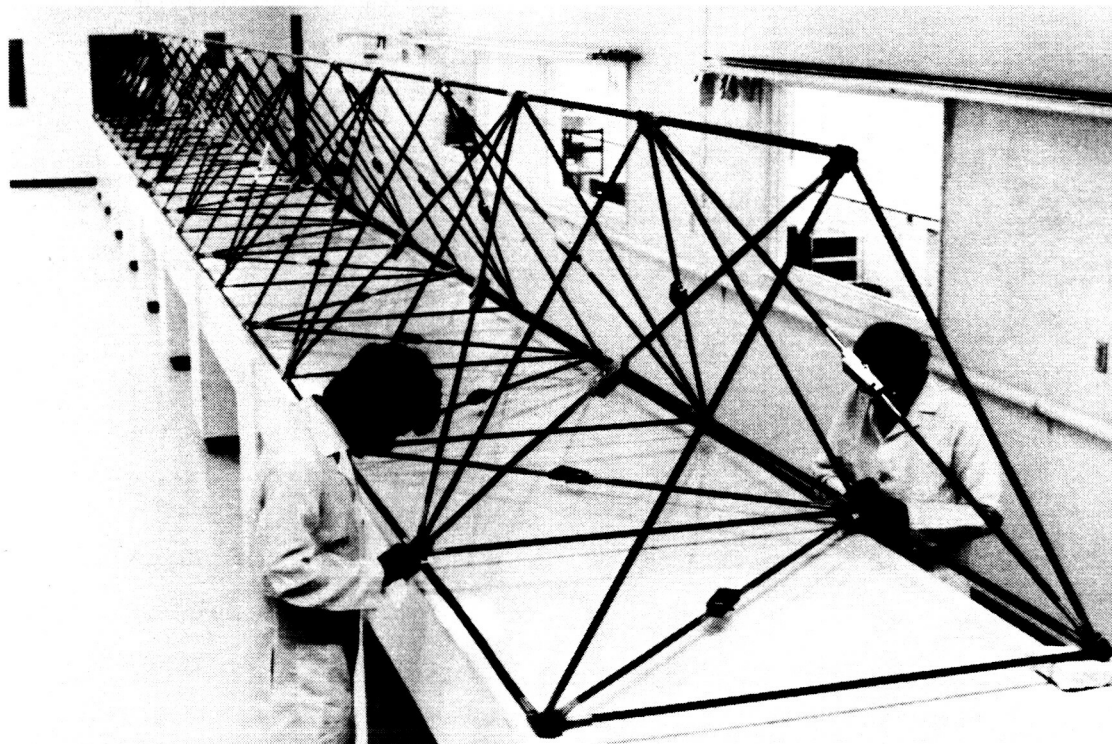
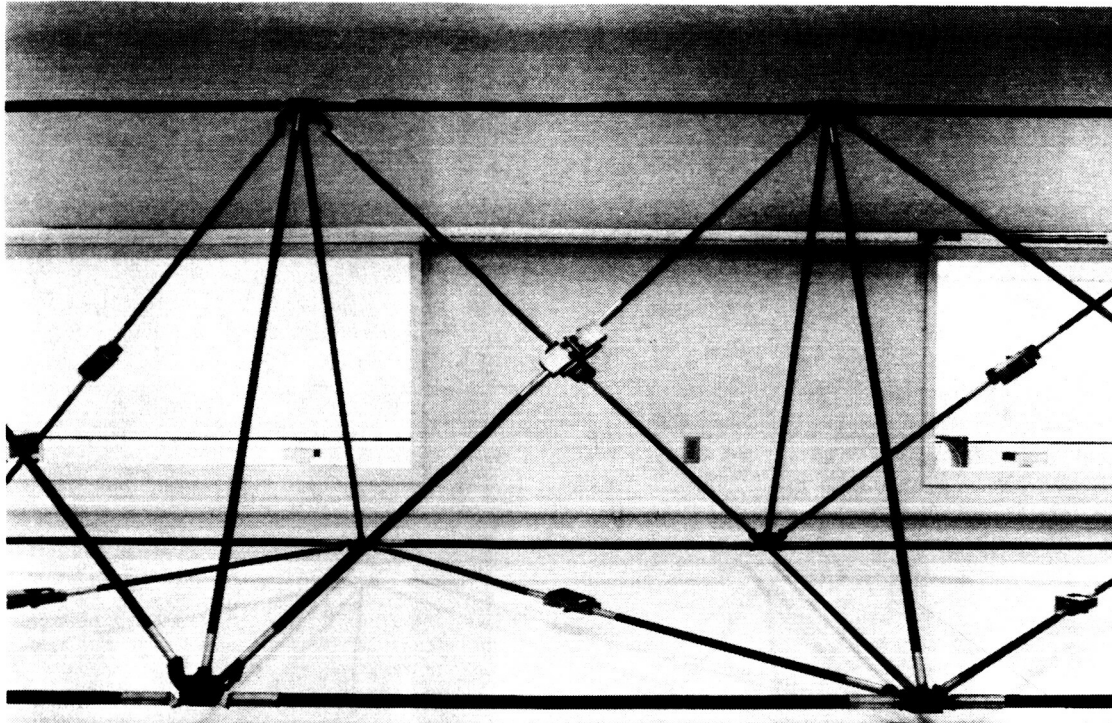


Figure 24. Full deployment of assembled beam.

## SECTION 5

### SUMMARY, CONCLUSIONS AND RECOMMENDATIONS

#### 5.1 SUMMARY

The truss beam is a robust, efficient structure which has been designed to meet the requirements of the truss beam model with substantial margins and safety factors. High modulus graphite/epoxy tubes are used for all lineal strut members, and precision titanium parts are used in the hinge hardware. The bending strength of 4,000 Nm includes a safety factor of 1.4 and meets the specified loading requirement with a positive margin. The bending stiffness of the beam assembly, including joint compliances, is  $1.15 \times 10^7 \text{ Nm}^2$  with a ten percent margin over the requirements. The lowest torsional vibration frequency is 4.5 times the lowest bending frequency. The coefficient of thermal expansion will vary with temperature, fiber batch, and environmental history, but should stay below an absolute value of  $0.5 \times 10^{-6}/\text{K}$ . The total mass of the 20.3-meter-long beam is near 95 kilograms, including end fittings and features to enhance resistance to ground handling. The result is a structure that is typical of high-quality spaceflight hardware.

The beam meets all of the secondary beam requirements including provisions for a wire harness, test components and electrical conductivity along the surfaces and length. The beam is easily repairable with hand tools, and each type of subassembly is interchangeable. Provisions have been included in the design for very stiff attachments to an end mass and to a base fixture.

#### 5.2 CONCLUSIONS

The truss beam as fabricated should exhibit the properties as set forth in Section 2.2. Deployment by single-degree-of-freedom hinges is possible, where in most cases the hinge angles are reasonable in terms of machining. Material strain and resulting moments during deployment are not excessive, but may be a problem if stiffer members are used, since deployment loads and fitting mass requirements increase, or if materials of lower strain limit are used, since safety margins would decrease.

The configuration and design of this beam have been guided by the desirability of predictable linear behavior. It is an excellent choice for a ground test article that is representative of future structures that will be used in space.

## REFERENCES

1. NASA Langley Research Center. "Statement of Work: Deployable/Retractable Truss Beam Model," No. 1-109-8200.0023, Exhibit B. Hampton, Virginia, 5 February 1985.
2. Roark, R.J., and W.C. Young. Formulas for Stress and Strain, 5th ed. McGraw-Hill Book Company, San Francisco, California, 1975.
3. Hedgepeth, J.M., and L.R. Adams. "Design Concepts for Large Reflector Antenna Structures: Final Report," ARC-TN-1117. Astro Research Corporation, Carpinteria, California, 19 August 1982.
4. Miller, R.K., J.M. Hedgepeth, and L.R. Adams. "Final Report: Geometric Studies of the Precision of Doubly Curved Reflector Surfaces Supported by Sequentially Deployed Trusses," ARC-TN-1118. Astro Research Corporation, Carpinteria, California, 24 August 1983.
5. Adams, L.R., and A. von Roos. "Stacbeam II: Final Report, Phase VI," ARC-TN-1134, prepared under Jet Propulsion Laboratory Contract No. 955847. Astro Aerospace Corporation, Carpinteria, California, 23 April 1985.
6. Adams, L.R. "Study of Efficient Structures for Geosynchronous Spacecraft Solar Arrays, Phase VII: Final Report," AAC-TN-1148. Astro Aerospace Corporation, Carpinteria, California, 19 September 1986.

# Standard Bibliographic Page

1. Report No. NASA CR-178287		2. Government Accession No.		3. Recipient's Catalog No.	
4. Title and Subtitle Design, Development and Fabrication of a Deployable/ Retractable Truss Beam Model for Large Space Structures Application				5. Report Date June 1987	
				6. Performing Organization Code	
7. Author(s) Louis R. Adams				8. Performing Organization Report No. AAC-TN-1150, Rev. A	
9. Performing Organization Name and Address Astro Aerospace Corporation 6384 Via Real Carpinteria, CA 93013-2993				10. Work Unit No.	
				11. Contract or Grant No. NAS1-18013	
12. Sponsoring Agency Name and Address National Aeronautics and Space Administration Langley Research Center Hampton, Virginia 23665				13. Type of Report and Period Covered Contractor Report	
				14. Sponsoring Agency Code	
15. Supplementary Notes  Langley Technical Monitor: Marvin D. Rhodes Final Report					
16. Abstract  A deployable/retractable truss beam model was designed and fabricated for use as a ground test article for the Control of Flexible Structures (COFS) program. This beam of high stiffness and strength has design features which facilitate linear analytical modeling of bending, axial and torsional loads. It is a statically determinate structure, 20 meters in length and 1.4 meters in diameter, which deploys using single-degree-of-freedom hinges from a packaged length of less than 3.5 percent of its deployed length.  The report discusses overall and specific design requirements, beam analysis including performance, hinge specification, deployment, kinematics and loads, design, fabrication and assembly.					
17. Key Words (Suggested by Authors(s))  truss beam deployable retractable hinge			18. Distribution Statement  Unclassified - Unlimited		
19. Security Classif.(of this report) Unclassified		20. Security Classif.(of this page) Unclassified		21. No. of Pages 65	
22. Price					

For sale by the National Technical Information Service, Springfield, Virginia 22161